EFFECT OF CHANNEL DEEPENING ON TIDAL FLOW AND SEDIMENT TRANSPORT;
PART II: MUDDY CHANNELS

Leo van Rijn; LeoVanRijn-Sediment Consultancy; Blokzijl, The Netherlands; info@leovanrijn-sediment.com and Bart Grasmeijer; Deltares, Delft, The Netherlands; The Netherlands; bart.grasmeijer@deltares.nl;

abstract
Natural tidal channels often need deepening for navigation purposes (larger vessels). The depth increase may lead to tidal amplification, salt intrusion over longer distances and increasing sand and mud import. Increasing fine sediment import, in turn, may start a process in which the sediment concentration progressively increases until the river becomes hyper-turbid, which may lead to increased dredging volumes and to decreased ecological values. These effects can be modelled and studied using detailed 3D-models. Reliable simplified models for a first quick engineering evaluation are however lacking.
In this paper we apply both simplified and detailed 3D models to analyze the effects of channel deepening in prismatic and weakly converging tidal channels with saturated mud flow. The objective is to gain quantitative understanding of the effects of channel deepening on mud transport. We developed a simplified tidal mud model describing most relevant processes and effects in saturated mud flows with only minor horizontal transport gradients (quasi uniform conditions). The simplified model is not valid for non-saturated mud flow conditions. This model can either be used in standalone mode or in postprocessing mode with computed near-bed velocities from a 3D hydrodynamic model as an input. The standalone model has been compared to various field data sets. Mud transport processes in the mouth region of muddy tidal channels can be realistically represented by the simplified model, if sufficient salinity and sediment data are available for calibration. The simulation of tidal mud transport and the behavior of an estuarine turbidity maximum (ETM) in saturated and non-saturated mud flow conditions cannot be represented by the simplified model and requires the application of a detailed 3D-model.
Keywords: tidal mud transport; tidal sediment modelling; deepening tidal channels

1. Introduction

Most alluvial estuaries have a converging funnel-shaped planform with a decreasing width in upstream (landward) direction. Some channels have a more or less prismatic planform due to the presence of dikes and/or groins to keep the channel velocities relatively high, preventing excessive siltation. However, the passage of large vessels often requires the dredging of relatively large depths of 10 to 20 m (larger than the natural depth), resulting in siltation and frequent maintenance dredging. Typical examples in Europe are: tidal Elbe River in Germany (BAW 2006; Kerner, 2007); Tidal Ems River in Germany (Talke et al. 2009; Van Maren et al., 2015a,b); Loire River in France (Walther et al., 2012); Western Scheldt tidal estuary (Winterwerp et al. 2013) and the Rotterdam Waterway (Rhine river mouth) in The Netherlands (Arcadis, 2015).
The focus point of this paper is the transport of mud, which can occur in three modes, as follows:
(i) non-saturated mud transport in conditions with mud percentages in the bed < 30% (supply-limited conditions);
(ii) saturated mud transport in conditions with percentages of mud in the bed > 70% (bed-dominated conditions, Bagnold 1962; Winterwerp 2006; Van Rijn 2007; more details in Section 3.3);
(iii) over-saturated mud transport in conditions with a large input of mud from upstream in combination with hindered settling effects resulting in hyper concentrations (supply-dominated conditions; Xu 1999a,b; Winterwerp 2006; Van Rijn 2007; Van Maren et al. 2009a,b; not studied in this paper).
In muddy tidal environments with non-saturated and saturated mud transport, an estuarine turbidity maximum (ETM) is often generated. The ETM is a zone of increased sediment concentration that occurs in river-dominated estuaries with stratified flow, where it influences the morphodynamic development of the bed (navigability and dredging), (see review of Jay et al. 2015). The mechanisms behind ETM particle trapping are qualitatively understood (Jay and Musiak 1994; Jay et al. 2015), but accurate quantitative predictions are still difficult. The most important mud transport processes involved are:
(i) advective transport processes due to river flow and tidal flow supplying mud from riverine and marine sources;
(ii) tidal asymmetry of velocities and mixing (eddy viscosity); flood values being significantly larger than the ebb values resulting in net landward mud transport;
(iii) horizontal gravitational circulation due to residual landward-directed near-bed flow and seaward-directed near-surface flow generated by longitudinal salinity-related density differences resulting in net landward transport of mud in the near-bed zone (Hansen and Rattray, 1965; Chatwin, 1976; Festa and Hansen, 1978, Prandle, 1985; Kuijper and Van Rijn, 2011);
(iv) tidal straining enhancing the landward near-bottom flow and mud transport due to variation of stratification and mixing during flood and ebb and over the neap-spring cycle (also known as sips: strain-induced periodic stratification effects); stratification is less during flood and near-bed mixing is stronger during flood (Simpson et al., 1990); Burchard and Baumert (1998) have shown that this process can be more important than gravitational circulation;

(v) suppression of turbulence at the interface of saline and fresh water in stratified flow (Geyer 1993, Geyer et al., 2000) resulting in the transport of fluvial fine sediments suspended in the fresher, upper parts of the water column into the layer beneath the pycnocline (De Nijs 2012) and

(vi) lag effect in muddy regimes; temporal lag (or scour lag) being the delayed response of mud concentrations to changing flow velocities and bed-shear stresses and spatial lag (or settling lag) related to the time and distance for sediment particles to settle out from the water column resulting in net horizontal transport of mud as the water depth and the settling distance are larger during HW slack than during LW slack and the landward decrease of the flow velocities; these processes are enhanced by differences in critical bed-shear stress for deposition and erosion (biological, consolidation effects), (Postma, 1954, 1961; Van Straaten and Kuenen, 1957; Groen, 1967; Dyer 1986; Chernetsky et al., 2010), although this concept is argued in various papers (Sanford and Halka 1993; Gatto et al. 2017).

Many studies show that the location of the ETM with relatively high suspended mud concentrations coincides with the location of the (moving) salt wedge (see overview by De Nijs, 2012). Mathematical computations using semi-analytical models for idealized cases (Talke et al., 2009; Chernetsky et al., 2010) and detailed numerical models (Burchard and Baumert, 1998; Van Maren et al., 2015b) confirm that mud is carried in landward direction by tidal velocity asymmetry (tidal pumping) in combination with density-driven residual flows near the bed (gravitational circulation; sips-effect). These processes are sufficient to maintain an ETM with relatively high mud concentrations with minimum supply from the local bed (non-saturated mud flow over a sandy bed).

Channel deepening, straightening as well as reclamation of the intertidal areas lead to changes of the hydrodynamic system: tidal penetration and salt intrusion over longer distances, tidal amplification with larger tidal ranges, increase of tidal velocity asymmetry and density-driven residual flow (Amin, 1983; DiLorenzo et al., 1993; Familkhalili and Talke, 2016; Talke et al., 2009; Chernetsky et al., 2010; Van Maren et al., 2015b; see Part I).

Channel deepening may lead to an increase of suspended sediment concentrations, larger transport and deposition rates, as discussed for the Ems river by Talke et al. (2009), Chernetsky et al. (2010), Winterwerp (2011), Winterwerp and Wang (2013), De Jonge et al. (2014) and Van Maren et al. (2015a,b). The increasing flood-dominated asymmetry strengthens various sediment importing mechanisms in the Ems river related to resuspension, vertical mixing and flocculation (Winterwerp, 2011) and lag effects (Chernetsky et al., 2010). Recent semi-analytical model studies show the up-estuary shift of the ETM due to channel deepening, changes in tidal asymmetry and bed roughness reduction due to the presence of fluid mud for the Ems river (Chernetsky et al., 2010; De Jonge et al., 2014).

Various papers (Winterwerp, 2011; Winterwerp and Wang, 2013; Van Maren et al 2015b) point to the risk of a regime change from non-saturated to saturated mud transport due to channel deepening, if sufficient mud is available in the system (Loire, Ems). Saturated mud flow in relatively deep channels may lead to the formation of fluid mud with a very smooth surface promoting tidal penetration and amplification (less flow resistance).

Most papers focus on site-specific muddy tidal channels. General conclusions on the relative importance of the trapping mechanisms involved are not always possible as the relative contribution of the trapping mechanisms may differ per estuary, and/or may change in time as a response to human interventions. The present paper has a more general approach focussing on the functional relationship between various important parameters (salt intrusion, residual velocity, mud transport) and the water depth for schematic cases of prismatic and converging channels.

Relevant questions addressed in this paper are: what is the effect of channel deepening on the salinity and sediment transport characteristics in tidal channels with mud and mixed sand-mud beds? How is salinity intrusion, residual velocity (estuarine circulation) and mud transport influenced by water depth? Is there a risk of regime change from export to import of sediment (or vice versa), under what conditions and what are the net tide-integrated mud transport rates involved? The attention is mainly focussed on prismatic channels based on the Rotterdam Waterway as an example, but converging channels (Ems and Elbe rivers in Germany) are also addressed.

The tidal Rotterdam Waterway in the Netherlands and the Elbe River in Germany are examples of stratified non-saturated mud flow over a partly sandy bed, whereas the small-scale tidal Ems River is an example of saturated mud flow over a smooth muddy bed. The most important characteristics of these tidal transport systems are discussed in Section 2 to identify the basic similarities and differences. The data available for these systems are used to validate detailed numerical models and simplified models for saturated and non-saturated mud transport described in Section 3. The application of a simple mud transport model (TMUD) that can used as standalone model is meaningful for the analysis of measured data and quick-scan feasibility studies. The TMUD-model can be coupled (post-processing) to a 3D hydrodynamic model for quick sensitivity studies to identify the most influencial parameters and processes.

Section 4 describes the application of a detailed 3D numerical model (Delft3D) to simulate the generation of an ETM in the Rotterdam Waterway with a partly sandy bed and to assess the effect of channel deepening on the behaviour of the ETM.

Finally in Section 5, the simplified tidal mud transport model (TMUD) is used as a standalone model to compute the net tide-integrated mud transport in the mouth region of a tidal channel for a range of conditions. The net tide-integrated mud transport rates are presented in a general plot as function of unit river discharges and water depths, which has not been done before. The transport data of the Ems river, Elbe river and Rotterdam Waterway (Section 2) are used to validate the computed results. The plot explains the regime shift from export to import of mud and can be used for a first engineering assessment of the effect of channel deepening (increased dredging) in muddy tidal channels. This type of information is not yet available and provides both qualitative and quantitative insights in channel deepening effects on mud transport processes.

2. Basic mud transport processes in tidal systems

If the fresh water river discharge in a tidal channel is sufficiently large and the mixing is relatively small, the tidal system is stratified with density-driven residual flow near the bed in landward direction. The combined velocities of river, tidal and density-driven flows are often sufficient to mobilize sand and mud from the bed, from the side slopes and from the banks to be transported up and down the tidal channel. The transport of mud consisting of very fine (cohesive) particles < 63 μm can occur at two modes: saturated and non-saturated conditions. Saturated mud transport with depth-averaged concentrations larger than about 1 kg/m^3 generally occurs in the case of a muddy channel bed, slopes and banks. Mud is then so abundantly available that the water column is fully saturated with fines (Bagnold, 1962; Xu, 1999a,b; Winterwerp, 2001). Non-saturated mud transport (wash load) with depth-averaged concentrations smaller than about 1 kg/m^3 mostly occurs in conditions with a mixed sand-mud bed. This latter type of mud transport partly depends on the far-field sources of mud. An estuarine turbidity maximum (ETM) can be generated in both types of regimes (saturated and non-saturated conditions). Sometimes, the entrainment/erosion capacity of the flow is too low (particularly during neap tides) to remove the mud from the bed which may lead to the (temporary) formation of a (fluid) mud bed.

We analysed and compared three different tidal systems with stratified flow: Ems and Elbe Rivers in Germany; Rotterdam waterway in The Netherlands. Characteristic features of these three systems are summarized in **Table 1**. The mud load and transport data of **Table 1** are crude estimates based on available data. These data are used in Sections 4 and 5 for order of magnitude verification of the detailed and simplified models.

2.1 Saturated mud transport in Ems River, Germany

An example of a funnel-type tidal channel with saturated mud flow is the Ems River landward of Pogum in Germany, which is extensively described in many papers (Herlling and Niemeyer, 2008; Talke et al., 2009; Chernetsky et al., 2010; Winterwerp, 2011, Herlling et al., 2014; Van Maren et al., 2015b). The studies of Talke et al. (2009), Chernetsky et al. (2010) and Van Maren et al. (2015a,b) show that channel deepening enhances the mud transport in the upper estuary due to increased tidal asymmetry and density-driven estuarine circulation.

The Ems tidal system consists of the Ems estuary seaward of Pogum and the Ems tidal River landward of Pogum. The length of the river upstream op Pogum is about 350 km. A weir is present in Hebrum, which is about 15 km upstream of Papenburg. The channel width in the mouth region Knock-Pogum, where a long training wall is present, varies between 400 and 650 m. The river width is about 650 m at Pogum and about 65 m just upstream of Hebrum. The tide propagates up to the weir at Hebrum. The tidal range at Pogum is about 3.4 m and at Papenburg about 3.6 m (amplification) and the river discharge varies between 30 and 250 m^3/s with a long-term mean value of about 80 m^3/s (Chernetsky et al., 2010; Van Maren et al., 2015b). Mud is abundantly available in the Ems estuary (downstream of Pogum) and Ems River. Data from Talke et al. (2009), Chernetsky et al. (2010), Winterwerp (2011) and De Jonge et al. (2014) show a pronounced ETM over a distance of about 50 km landward of Leer (Leer is about 20 km upstream of Pogum). Large mud concentrations have been measured in the ETM with values of 50 kg/m^3 at 0.5 m above bed, 20 kg/m^3 at 1 m above bed, 10 kg/m^3 at 2 m above bed and 1 kg/m^3 at 5 m above bed. Depth-averaged values are in the range of 1 to 3 kg/m^3. Given these values and flood dominated tidal velocities of 1 to 1.3 m/s in the river section Pogum to Leer, the net tide-integrated mud transport in the section Pogum-Leer is of the order of 5 ton/m/tide in landward direction (import for low river discharge < 0.3 m^2/s).

Van Maren et al. (2015 a,b) computed the tidal flow and mud concentrations for the bathymetry of 1945 (small depths < 5 m) and of 2005 (larger depths of 5 to 10 m). In 1945, the river bed was sandy with a Manning coefficient of n= 0.015 to 0.02 (Chézy-value= 60 to 80 m$^{0.5}$/s). In contrast, the river bed in 2005 was muddy with n = 0.01 (Chézy-value= 100 to 150 m$^{0.5}$/s). The increase of the water depth and the decrease of the bed roughness have not had much effect on the peak tidal flood and ebb velocities in the mouth region (Van Maren, personal communication 2015, see Figure 11 of Van Maren et al. 2015b). The computed peak tidal bed-shear stresses in 2005 were found to be smaller than those in 1945 mainly due to the smaller Manning-coefficient. River flushing velocities in 2005 were smaller due to the larger water depths. The model results showed much larger (factor 5) mud concentrations in 2005 than in 1945. The total tide-averaged suspended mud load in the ETM zone of the lower Ems River in 1945 was about 30x10^3 ton (150 ton/m; river width≅ 200 m), which increased to about 150x10^3 ton (750 ton/m) in 2005. The most important features are summarized in **Table 1**.

2.2 Non-saturated mud transport in Elbe River, Germany

The Elbe River originates in the mountains of the Czech Republic and flows through Germany over 630 km passing the city of Hamburg (largest German seaport) at about 110 km from the mouth at Cuxhaven (**Figure 1**). The fresh water river discharge varies between 200 and 3600 m³/s with a mean value of about 700 m³/s (BAW, 2006; Kerner, 2007). The mouth of the estuary is characterized by a narrow deep channel and wide tidal flood plains (Hakensand, Medem sand, Norder Grunde). The total width of the mouth at Cuxhaven is about 15 km. The width of the tidal river landward of Brunsbüttel is about 1500 to 3000 m. The width of the navigation channel (dredging width) varies between 400 and 600 m. The cross-sections of the tidal river at the mouth are about 20,000 to 40,000 m². Presently, the water depth is about 15 m below LAT up to Hamburg. The Port of Hamburg is planning to increase the water depth between the river entrance and Hamburg.

The tide penetrates over about 140 km up to the weir at Geesthacht (about 30 km upstream of Hamburg). The weir is generally closed for discharges smaller than about 1200 m³/s. The tidal range is roughly constant with a value of 3 m (springtide) up to Stadersand at 70 km from the mouth at Cuxhaven, after which the tidal range gradually increases to about 3.7 m at Hamburg. Landward of Hamburg the tidal range gradually decreases to a value of 2 m at the weir of Geesthacht. The reduction of the tidal range between Hamburg and Geesthacht is mainly caused by the reduction of the water depth from 15 m to about 5 m (damping due to flow resistance; BAW 2006). Model computations by BAW (2006) show that the peak tidal velocities between the river mouth Brunsbuttel and Hamburg gradually decrease in landward direction with exception of the region between Stade and hamburg (**Figure 1**) during flood tide, which is caused by the local planform (abrupt change of the width) of the river.

The bed of the navigation channel along the Elbe River mainly consists of fine and medium sand with a d_{50} of about 250 to 350 μm (BAW, 2006). Large sand waves are present along the bed of the tidal Elbe River with heights in the range of 1 to 3 m and lengths in the range of 50 to 150 m (Van Rijn, 1993; BAW, 2006). The channel slopes consist of fine sand, silt and mud. The shallow areas near the banks mainly consist of silt and mud, particularly in the ETM near the ferry Wischhafen-Glückstadt at about 50 km from Cuxhaven. The tidal flats in the outer estuary mainly consist of fine sand with patches of silt and mud.
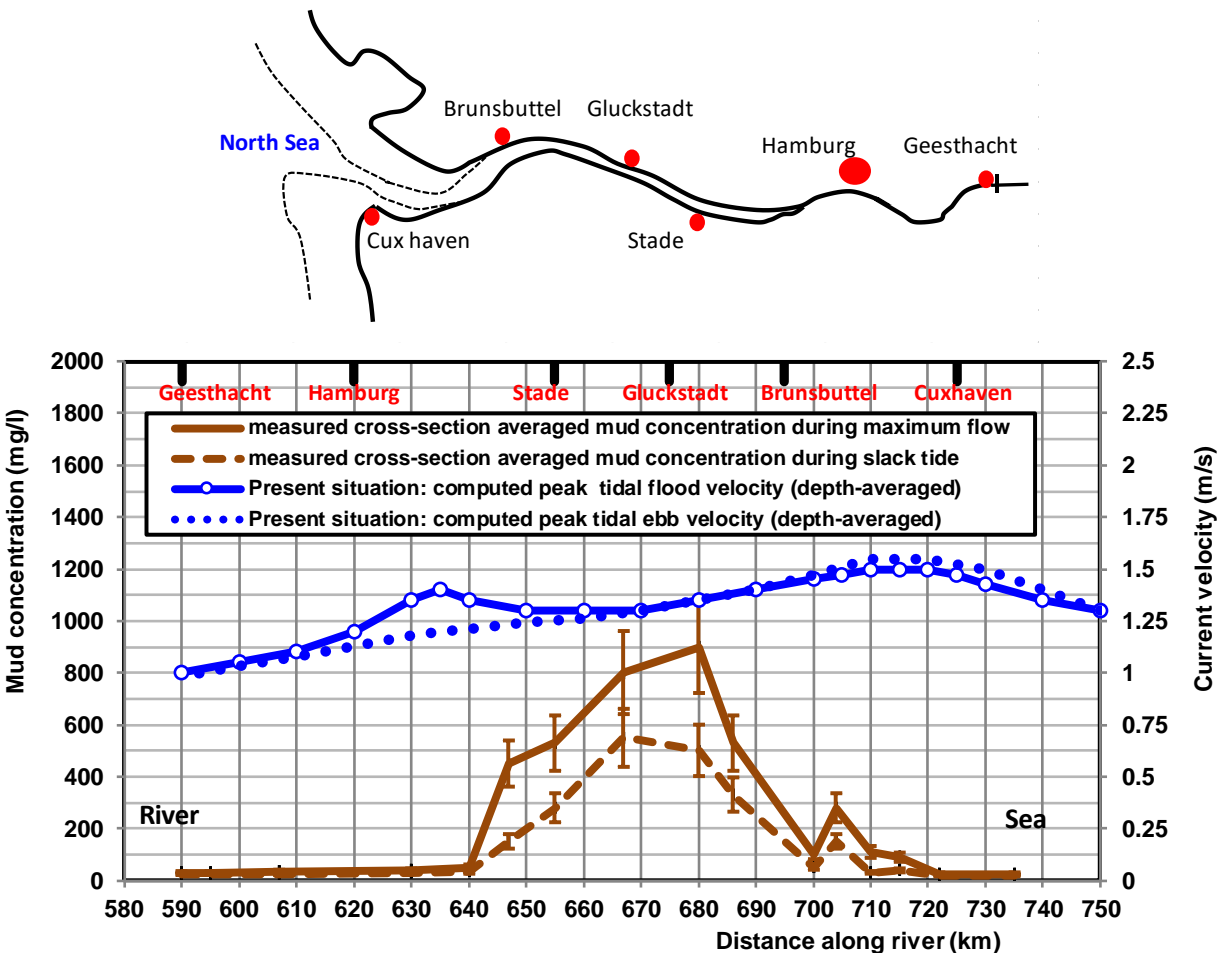
Figure 1   *Observed mud concentrations and computed peak tidal velocities (lower) in turbidity zone of Elbe tidal channel (upper) during neap-spring in May 2002 (derived from data of BAW 2006)*

4

Figure 1 shows the cross-section-averaged mud concentrations of the ETM between Brunsbuttel km 695 near the mouth and Hamburg-West km 620 based on detailed field surveys in 2002 in 15 cross-sections (BAW, 2006). The mud concentrations were derived from the backscattered signal of ADCP-profiles calibrated with many water-sediment samples. The salt intrusion reaches Stade km 655 (70 km from Cuxhaven). The ETM has a bell-shaped concentration distribution with landward increasing concentrations to a maximum followed by decreasing concentrations towards the salinity head. The mud concentrations are maximum (values between 400 and 1000 mg/l) around the location of the ferry Wischhafen-Glückstadt.

At the mouth near Cuxhaven the mud concentrations are about 50 to 100 mg/l (BAW, 2006). The md concentrations in the river landward of Geesthacht (weir) are about 50 mg/l (BAW, 2006). The data are characteristic for the present situation as the tidal flow and the salinity system have not changed much since 2002. Most of the mud in the ETM is continuously supplied by net tidal import due to density-driven flows near the bed and to a lesser extent by mud supplied from the river upstream of Geesthacht.

During slack tide, the mud flocs with relatively high settling velocities can accumulate at the channel bed and at the relatively shallow side slopes and banks of the ETM in a thin layer (<0.03 m). This layer can easily be removed from the sandy channel bed during maximum flow with velocities > 1 m/s. However, the smaller velocities on the side slopes and banks result in the gradual accumulation of mud here. This can only be removed by dredging or occasionally by erosion during high river runoff events.

No major harbour basins are located along the ETM between Brunsbüttel and Hamburg-West, which means that there are no human-induced mud sinks along this stretch. Based on the available data from BAW (2006), we estimate the total amount of mud accumulated in the ETM at about 200,000 ton or about 400 ton/m (width of navigation channel $\cong$ 500 m).

The total amount of annual dredging in the Elbe River is about 4000 ton/tide:

(i) ETM between Brunsbüttel and Hamburg-West: about 5 million m^3/year in the period 2001-2005 (BAW, 2006) or about 2000 ton/tide (730 tides per year; bulk density of 0.3 ton/m^3);

(ii) Hamburg harbour docks: about 2000 ton/tide in the period 2001-2005 (BAW, 2006).

The total annual amount of mud supplied by the long-term mean river discharge of 700 m^3/s with a long-term mean mud concentration of 50 mg/ is about 1 million ton per year or about 1500 ton/tide (assuming 730 tides per year). This means that 4000 -1500 = 2500 ton/tide has to be supplied at the Brunsbüttel side of the ETM by the tidal transport processes to maintain the 'equilibrium' mud load of the ETM. The dredged materials are dumped in the outer estuary far beyond Brunsbuttel. These estimates are order of magnitude estimates but are sufficiently accurate to identify the relative contribution of the different sources. **Table 1** summarizes the most important data. Transport rates are given in ton/m/tide for reasons of comparison.

2.3   Non-saturated mud transport in prismatic Rotterdam Waterway, The Netherlands

An example of non-saturated mud transport over a sandy channel bed is the nearly prismatic Rotterdam Waterway in The Netherlands (see **Figure 1** of Part I). The Rotterdam Waterway is the main tidal navigation channel (width of about 500 m) to the Port of Rotterdam at about 30 km from the mouth (between the jetties). It is the artificial mouth of the Rhine River in the North Sea. The Rotterdam Waterway is a narrow prismatic channel (width $\cong$ 400 to 600 m) with a staircase-type longitudinal bottom profile with water depths increasing in steps from 18 m at the mouth to 11 m at Rotterdam (Arcadis, 2015). A storm surge barrier (Maeslant barrier) that can be closed in extreme storm conditions is present at about 8 km from the mouth in a section with slightly reduced depth and width. Further upstream at 21 km from the mouth, a side branch is present (Old Meuse River). Many docks are present along the Waterway; new docks near the mouth and older docks near the city of Rotterdam. The Port of Rotterdam is planning to increase the water depth from 15 m to 16.3 m in the region between the mouth km 1030 and km 1010 (Arcadis, 2015). The depths between the mouth km 1035 and 1030 is with 18 m already sufficiently large. The Port of Rotterdam is planning to make a major local adjustment of the planform of the tidal channel at km 1030 where the entrance to the southern Calland channel is realigned. All basic data of the Rotterdam Waterway have been taken from Arcadis (2015) and De Nijs (2012).

The nearshore zone, coastal waters and the beaches near the mouth of the Waterway consist of sandy materials (d_{50} = 0.1 to 0.3 mm) with little mud (<5%). The channel bed consists of fine to medium sand (d_{50} = 0.2 to 0.4 mm), with the coarser fraction near the mouth between km 1035 and 1025 and the finer fraction further upstream between km 1025 and 1010. The percentage of mud gradually increases from 5% at the mouth km 1035 to 10% at km 1015 and to 35% at km 1010. Patches of gravel are present locally as relict features of former channel bed stabilization activities.

The fresh water river discharge varies seasonally between about 500 and 5000 m^3/s with an annual mean of about 1300 m^3/s. The tidal system is strongly stratified with salt intrusion over about 20 km. The tidal range varies from about 2 m at the mouth to almost zero at 70 km upstream due to bottom friction (damped tide). The tidal flow near the mouth is ebb-dominated in the upper part of the water column with peak ebb velocities of about 1.5 to 2 m/s and flood-dominated in the lower part with peak flood velocities of 1 to 1.5 m/s. The tide-averaged density-driven residual flow velocities near the bed are 0.2 to 0.3 m/s indicating strong gravitational circulation, particularly in the winter period, which is the time when the near-bed sediment concentrations at sea are relatively high.

The annual deposition and dredging of sand and mud along the Rotterdam Waterway is confined to four main regions (Arcadis, 2015), namely A) southern channel bed and harbour entrances in the mouth region (about 3 million m³/year of mud and 1 million m³ of sand from marine origin), B) harbour basins in the mouth region (about 3 million m³ of mud), C) the inland sandy channel bed (about 1 million m³/year of sand) and D) the inland harbour basins along the ETM zone (about 3 million m³/year of mud).

Hence, the total mud dredging volume in and near the harbour basins is presently about 9 million m³/year (Arcadis, 2015). Furthermore, major deposition takes place in the navigation channel at sea outside the mouth of the Waterway (about 2 million m³/year of sand).

The transport of mud along the Rotterdam Waterway can be characterized as non-saturated mud transport over a mainly sandy bed. Mud is supplied from the river, from sea and to a small extent from local sources (channel bed and banks). The fine sediments accumulating in the salt wedge are slowly carried to the salinity head by the combined near-bed tidal flood current and the density-driven near-bed current. The near-bed current velocities during flood are so strong that all fines deposited on the channel bed during slack water (only a very thin layer of 0.01 m if all mud from the water column is deposited) are eroded/entrained again. The measured tide-averaged mud concentrations in the turbidity zone of the Rotterdam Waterway during springtide at 11 April 2006 based on the data from De Nijs (2012) are shown in **Figure 2**. The tide-averaged mud concentrations in the region of 15-22 km from the mouth have a maximum value of about 40 mg/l near the water surface and 250 mg/l near the bed. The variations during a spring tidal cycle are shown. The high-concentration cloud of fines near the bed has a thickness of about 2 m and a length scale of about 7 km and moves up and down the tidal channel. During and after storm conditions (winter season), the depth-averaged mud concentrations from the sea may go up to about 200 mg/l and near-bed concentrations entering from the sea may be as large as 1000 mg/l (Rijkswaterstaat, 2000). During periods with large river runoff, the mud concentrations from the river may go up to about 200 mg/l (Asselman, 1997).
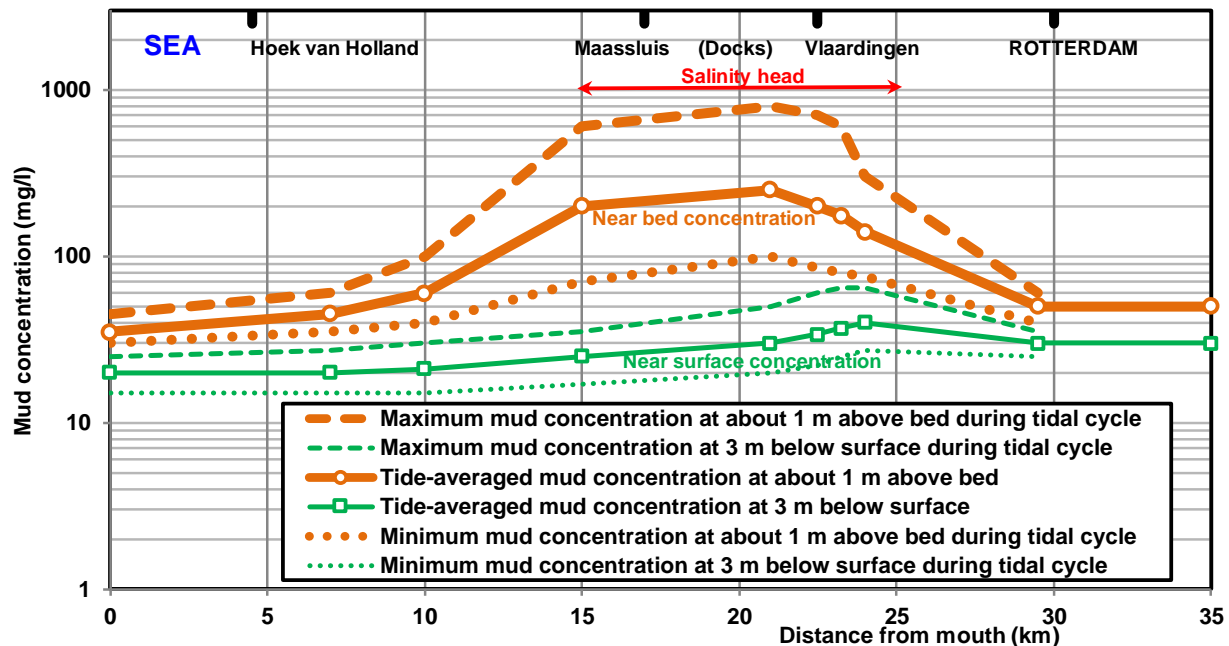
Figure 2 *Measured mud concentrations near the bed and near the surface in turbidity zone of Rotterdam Waterway during springtide; 11 April 2006; $Q_{river} \cong 1700$ m³/s; derived from data of De Nijs (2012)*

The total annual mud supply (< 63 μm) from the river upstream of Rotterdam is about 1 to 2 million ton/year or about 1300 to 2500 ton/tide based on 730 tides per year resulting in 2 to 5 ton/m/tide for a width of about 500 m (De Nijs, 2012; Arcadis, 2015). This is equivalent with an annual mean mud concentration of 15 to 30 mg/l from upstream of Rotterdam (De Nijs 2012). Erkens (2009) mentions a value of 3.5 million ton/year at the Dutch-German border. The trapping of fines imported from marine sources by density-driven near-bed flows and tidal pumping (velocity asymmetry due to deformation of tidal wave) is equally important (De Nijs 2012), but mainly occurs in and after storm conditions in the winter season with relatively high mud concentrations generated by seawaves in the nearshore zone just seaward of the Rotterdam Waterway mouth.

De Nijs (2012) shows that the flow pattern in the Rotterdam Waterway is largely determined by the combination of (barotropic) tidal velocity asymmetry and (baroclinic) density-driven flows near the bed and suppression of turbulence at the pycnocline (interface of saline and fresh water; see Geyer, 1993 and Geyer et al., 2000). Fine sediments that are in suspension in the fresher, upper parts of the water column settles into the layer beneath the pycnocline from where it cannot be re-entrained by turbulent mixing (De Nijs 2012). In this way the water column above the salt wedge is slowly cleared from suspended mud during the tidal cycle resulting in a decrease of suspended mud concentrations in seaward direction. De Nijs

(2012) estimated the tide-integrated mud transport rates at both ends of the ETM based on his data of 11 April 2006 with a relatively large fresh water discharge of about 1700 m³/s (annual mean=1350 m³/s). The tide-integrated mud input at the landward side of the ETM was found to be about 2500 ton/tide from the river and the tide-integrated mud output at the seaward end of the ETM was about 1500 ton/tide in seaward direction (mud export). This yields an overall deposition of about 1000 ton/tide in the ETM and surrounding docks/basins. This budget analysis indicates that the net supply of mud to the ETM is of fluvial origin at that date of 11 April 2006.

The total amount of mud accumulated in the ETM (**Figure 2**) with a depth of about 10 m, a width of about 500 m and a length of 15 km is about 10,000 ton, which is a relatively small value. Given the mud supply of 1300 to 2500 ton/tide from the river, the total mud load in the ETM can theoretically be replaced by mud from the river within 4 to 8 tides. Each tide about 1000 ton of mud (10% of the total mud load of the ETM; 40% to 70% of the river supply) is carried into the harbour basins along the ETM (De Nijs, 2012).

Mud import of marine sources mainly occurs in the winter period with wave stirring of mud present in the seabed (Winterwerp and Van Kessel 2003; Rijkswaterstaat 2000). The mud deposition in the mouth region (length of about 5 km) seaward of the ETM is mainly caused by flood-dominated import of mud from coastal waters in the winter period. The seabed generally consists of fine to medium sand ($d_{50} = 0.1$ to 0.3 mm) with low percentages of fines (<5%). Measured data from Rijkswaterstaat (2000) shows that the concentrations of fines entering the mouth during calm conditions are relatively low (10 to 30 mg/l). During and after storm conditions with surface waves of 2 to 3 m in waters of 10 to 20 m deep, the mud concentrations near the bed increase to values of about 1000 mg/l (Rijkswaterstaat 2000) in a layer of about 2 m thick due to stratification effects with damping of turbulence (little upward mixing). The depth-averaged concentrations may be as high as 200 mg/l. During the winter period, the fresh water outflow is relatively large resulting in density-driven residual flows near the seabed in landward direction that produce relatively high net mud transport rates (estimated to be about 10 ton/m/tide at the mouth in the winter season). This results in deposition of mud and fine sand (about 30% of the total annual deposition) in the mouth region as the surface waves will gradually decay between the harbor jetties. The deposition in the docks of the mouth region is relatively large in the winter period. The deposition of mud may result in the formation of local fluid mud layers with a thickness up to 3 m in certain areas (dock entrance areas) where the water depths are large and the velocities are low. As the water depths in the mouth region are considerably larger than those further inland, these fluid mud layers cannot migrate in landward direction against the longitudinal bottom slope.

Tidal and sediment transport parameters	Ems River	Elbe River	Rotterdam Waterway
Water depth below mean sea level in mouth region (m)	6-10	14-16	11-18
Navigation channel width in mouth region (m)	200-400	400-600	400-600
Tidal range (m)	3-3.4	2.8-3.2	1.8-2
Mean river discharge (m³/s) and unit river discharge (m²/s)	80; 0.2-1.2	700; 0.5-1.5	1300; 1-3
Peak tidal velocities in mouth region (m/s)	1-1.3	1.3-1.6	1-1.5
Bed composition in main channel (p_{mud}=percentage of mud)	muddy p_{mud}>70%	sand-mud p_{mud}=30-50%	sand-mud p_{mud}=5-35%
Bed composition at side slopes of main channel	muddy	muddy	sand-mud
Length of ETM (km)	40-60	40-60	15-20
Depth-mean mud concentration in upstream river (mg/l)	<30	30-50	30-50
Maximum depth-mean mud concentration during flood in mouth region (mg/l)	100-300	100-200	30-150
Maximum depth-mean mud concentration during flood in ETM (mg/l)	1000-3000	300-1000	50-150
Maximum mud load of ETM during flood per unit width $M_{load}= 0.7\ C_{ETM}\ L_{ETM}\ h_{ETM}$ (ton/m)	300-900	150-500	20-50
Flood-integrated mud transport during flood per unit width in mouth region $q_{mud,mouth,flood}= 0.7\ U_{mouth}\ C_{mouth}\ h_{mouth}\ \Delta t_{flood}$ (ton/m/floodtide)	20-80	30-100	5-35
Flood-integrated mud transport during flood per unit width in ETM $q_{mud,ETM,flood}= 0.7\ U_{ETM}\ C_{ETM}\ h_{ETM}\ \Delta t_{flood}$ (ton/m/floodtide)	200-600	100-300	10-30
Net tide-integrated mud transport per unit width (ton/m/tide; import)	2-8	3-10	4-8
Mud supply per unit width by upstream river (during one tide) $q_{mud,river}= U_{river}\ C_{river}\ h_{river}\ \Delta t_{flood}$ (ton/m/tide)	<1	2-5	2-5

U= velocity, C= mud concentration, L= length, h= water depth, Δt_{flood}= duration flood tide ($\cong$20,000 s)

Table 1 *Characteristic tidal and mud transport parameters of Ems, Elbe and Rotterdam Waterway (based on data from the references given in Sections 2.1, 2.2 and 2.3)*

Based on the presently available data (De Nijs, 2012; Arcadis, 2015), most likely there is export of mud during the spring and summer seasons and import of mud during the autumn and winter seasons. The estimate of the annual mud import at the mouth of the Rotterdam Waterway is about 6 millions m^3/year, which is equivalent to 6±2 ton/m/tide (based on a bulk density of 0.4 ton/m^3, width of 500 m and 730 tides per year).

2.4 Concluding remarks

Summarizing, the aforementioned examples show that an ETM can be generated in both saturated and non-saturated mud transport conditions. The Ems River is an example of saturated mud transport over a muddy bed with high-concentration mud layers and fluid mud layers in the bed zone, whereas the Elbe river is an example of non-saturated mud flow over a muddy sand bed. The mud concentrations in the ETM of the Elbe river are much smaller (factor 5) than those in the Ems River, but the mud loads of the ETM are very comparable due to the larger scale of the Elbe tidal system (**Table 1**). The mud transport during flood in the ETM of the Ems River is a factor of 10 larger than that in the mouth region. In the Elbe River, the mud transport during flood in the ETM is a factor of 3 larger than that in the mouth region, because much less mud is available in the top layer of the bed. In both the Ems and Elbe systems, the net tide-integrated mud import per unit width from marine source is of the order 5 ton/m/tide. In the Elbe system, the upstream (fluvial) mud supply is of the same order of magnitude as the mud import from marine sources. In the Ems system, the upstream (fluvial) mud supply is almost absent.

The ETM of the Rotterdam Waterway is much less pronounced with depth-mean concentrations of 50 to 150 mg/l. The total mud load of the ETM is only 20 to 50 ton/m, which is a factor of 10 smaller than that in the Ems and Elbe systems. The upstream mud supply (from the river) is of the order of 2 to 5 ton/m/tide, which is similar to that in the Elbe system. The net annual mud import at the mouth is not well known but based on available dredging volumes estimated to be in the range of 4 to 8 ton/m/tide (Arcadis, 2015). Storm events in the autumn and winter seasons have a relatively important effect on the mud import processes, whereas mud export processes may occur in the spring and summer seasons. Most of the mud from riverine and marine sources is trapped in the harbour basins along the Rotterdam Waterway requiring continuous maintenance dredging.

The data of these three tidal systems provide qualitative and quantitative insights into the response of an ETM to external forcing and the mechanisms behind ETM particle trapping. The percentage of mud present in the top layer of the bed is an important parameter to be measured during field surveys. A pronounced ETM requires a bed with at least 30% of mud at most places (Elbe River). The role of extreme events and altered flow regimes (water depth, bottom friction, turbulence damping, etc.) on trapping mechanisms and ETM dynamics is not fully clear. Jay et al. (2015) argue that an accurate prediction of an ETM is still not feasible but Talke et al. (2009) and Van Maren et al. (2015b) have shown that the ETM in Ems River can be successfully simulated by detailed semi-analytical and numerical models. We made an attempt to simulate the generation of an ETM in the prismatic Rotterdam Waterway using a 3D-model for non-saturated mud transport over a sand-mud bed (Section 4).

3. Models used

Here we use the Delft3D modelling suite (see Part I) and a simplified mud transport model (TMUD). Delft3D is an integrated modelling suite, which simulates two-dimensional (in either the horizontal or the vertical plane) and three-dimensional hydrodynamics, sediment transport, morphology, water quality and ecology and simulates the interactions between these processes. This detailed model includes all relevant processes along a varying bathymetry but it requires much longer run times than a simplified model. The simplified TMUD-model is a local model neglecting horizontal advection and diffusion of sediment. It can therefore not simulate the horizontal concentration distribution of the ETM but the short run times facilitate many sensitivity runs to gain insight in the different contributing processes (see Talke et al., 2009). Both detailed and simplified models are complementary.

The TMUD-model can be used as a standalone model or as a post-processing model using input from 2DH or 3D models such as Delft3D. The TMUD-model computes the vertical velocity profiles and mud concentration profiles as function of time over the tidal cycle at a fixed location in the mouth region of a tidal channel. An empirical function is used to generate the near-bed mud concentration based on the computed bed-shear stress. In standalone mode, the tidal velocity is assumed to be sinusoidal with prescribed asymmetry (input). The standalone model includes estuarine circulation (two-layer flow and residual velocities), which requires the horizontal salinity gradient as input. The net tide-integrated values are obtained by integration over the tidal cycle. In this paper we apply both the detailed Delft3D model and the simplified TMUD model to explore the change of tide-integrated mud transport as function of the water depth (channel deepening) in Sections 4 and 5.

3.1 Simplified salinity intrusion

The most important parameters influencing the salt intrusion length at the end of the flood period are the tidal characteristics (water level amplitude and peak tidal velocity at the mouth), the river parameters (discharge and cross-section averaged velocity) and the geometrical parameters (depth, width at mouth and convergence length scale).

Herein, the attention is focused on the maximum salt intrusion length occurring at high water slack (HWS) which is relevant for sediment transport processes. Analytical salinity distributions for prismatic and converging tidal channels proposed by

various authors are extensively discussed by Kuijper and Van Rijn (2011). Adopting a tide-averaged approach, the one-dimensional salt continuity equation can be expressed as a balance between the seaward-directed advective salt transport and the landward-directed dispersive or mixing-type transport, which can be described by analytical expressions. The method of Kuijper and Van Rijn is valid over a very wide range of conditions (depths 3 to 14 m; river discharge 10 to 10000 m^3/s; salt intrusion distance 30 to 150 km), based on comparisons of measured and computed salinity distributions for various tidal systems.

Figure 3 shows the computed maximum (at HW slack) salinity intrusion in a prismatic channel as function of the water depth and river discharge based on the well calibrated expressions given by Kuijper and Van Rijn (2011). Also shown is the measured salinity intrusion length of the prismatic Rotterdam Waterway (from ship-based measurements; Kuijper and Van Rijn, 2011) which refers to a depth of about 13 m and a river discharge of 1150 m^3/s or about 3 m^2/s (river width of 400 m). The computed values agree well with the observations. The salinity intrusion decreases for increasing river discharge. The salinity intrusion increases for increasing water depth because the tidal penetration is larger for a larger depth (less resistance). From **Figure 3** it can be derived that the salinity intrusion $L_s \sim h_o^{2.3}$ for $q_r = 1$ m^2/s and $L_s \sim h_o^2$ for $q_r = 5$ m^2/s. The effect of water depth on the salinity intrusion is stronger than for tidal penetration which is: $L_p \sim h_o^{1.5 \text{ to } 1.8}$ (see Part I). It is clear that the salinity intrusion increases for increasing tidal penetration, but the salinity intrusion depends on the horizontal dispersion processes which depend on the water depth. The simplest expression for salinity intrusion in prismatic channels is given by Van Os (1993) and Prandle (1985): $L_s \sim h_o^{2.5} C^2 B / (U_{max} Q_r)$ with C= Chézy-coefficient, B= channel width, U_{max}= peak tidal velocity and Q_r= river discharge. Assuming C, B, Q_r and U_{max} (see Part I) to be approximately constant for varying water depths, it follows that: $L_s \sim h_o^{2.5}$. Hence, an increasing water depth has a relatively strong effect on the salinity intrusion length and thus on estuarine circulation and mud transport (see Prandle 2009).

The model of Kuijper and Van Rijn (2011) provides the depth-averaged salinity distribution along a prismatic channel, as shown in **Figure 4** for 6 representative cases. The depth-averaged salt concentration at the sea boundary is set to 25 kg/m^3; measurements just outside the mouth of the Rotterdam Waterway show values in the range of 25 to 30 kg/m^3 over the tidal cycle. The salt concentration decreases monotonically to zero over the intrusion length. The horizontal density gradient of **Figure 4** varies roughly between $d\rho/dx \cong 0.01$ kg/m^3/m for a small depth ($L_{salinity} \cong 2.5$ km) and 0.0005 kg/m^3/m ($L_{salinity} \cong 55$ km) for a large depth. This gradient is the driving force for gravity circulation (secondary residual flow).

Based on measured data of the Rotterdam Waterway, the horizontal salinity distribution (except close to the sea boundary) can be reasonably well described with an error of about 15% to 20% by an exponential curve (concave) in prismatic channels with a pronounced salt wedge (see Figure 8 of Kuijper and Van Rijn, 2011). The model performance is less near the sea boundary where the computed density gradient is too large compared to the much smaller measured gradients. A more S-type curve occurs in tidal channels with a small river discharge as the vertical salinity profiles are more uniform due to tidal mixing processes (Delaware estuary, USA; Western Scheldt estuary, Netherlands; Kuijper and Van Rijn, 2011).
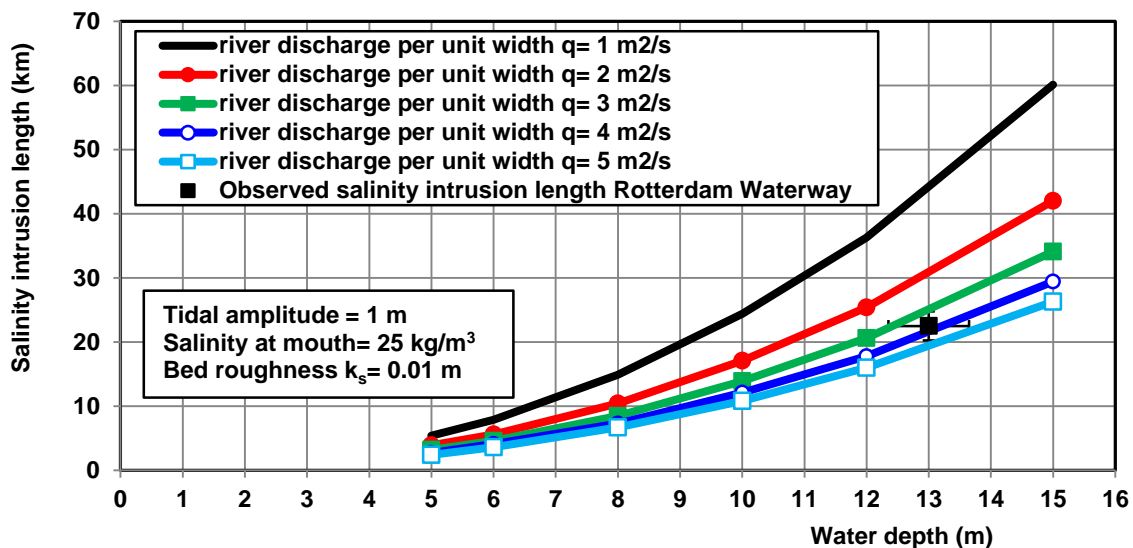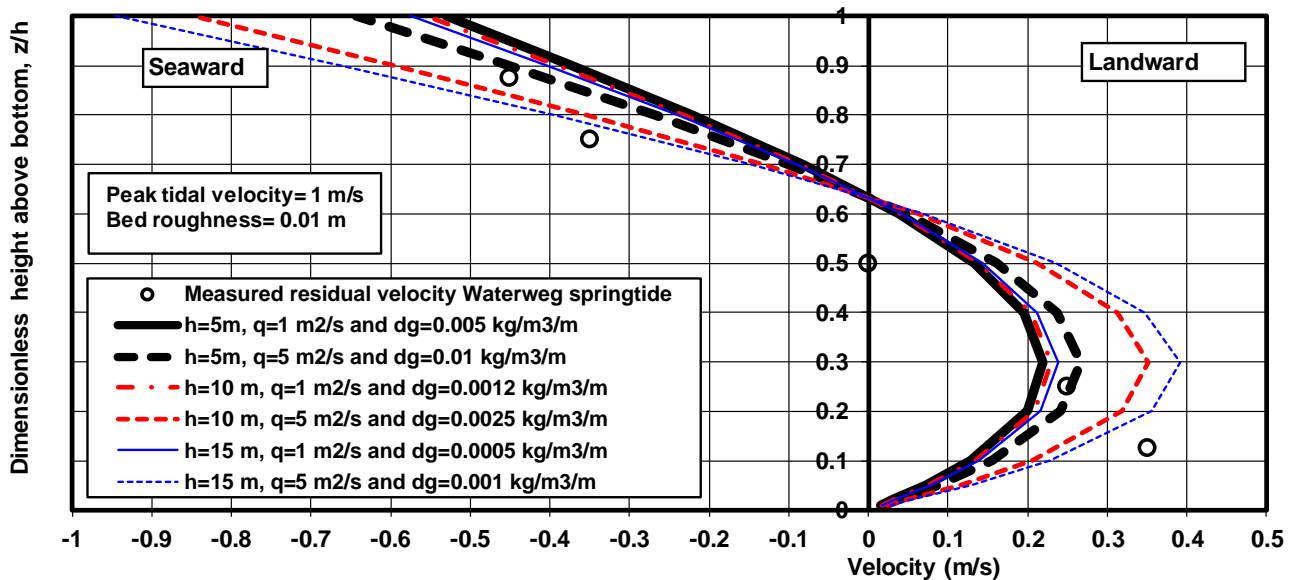

Figure 3   *Effect of water depth and river discharge on maximum salinity intrusion for prismatic channel (Tidal amplitude= 1 m; Salinity at mouth=25 kg/m³; Bed roughness= 0.01 m)*

9
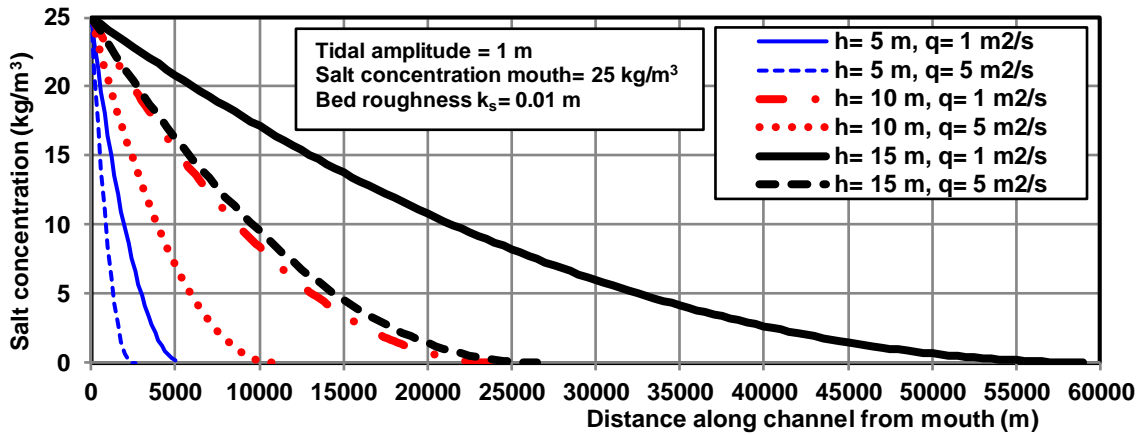
Figure 4 *Effect of water depth and river discharge on computed salinity distributions along a prismatic channel (Tidal amplitude= 1 m; Salinity at mouth=25 kg/m³; Bed roughness= 0.01 m)*

3.2 Density-induced circulation

An important process for the import of mud from marine sources is the density-driven residual velocity (Hansen and Rattray 1965; Prandle 1985, 2004, 2009), which can be computed by Equation (9) of Part I. This equation is most valid for the mouth region of a tidal channel with partially-mixed density profiles and is very similar to that of Hansen and Rattray (1965), Chatwin (1976) and Prandle (1985, 2004, 2009). The residual velocity profiles (based on Equation 9) for six representative cases of the Rotterdam Waterway are shown in **Figure 5**. These cases are: three water depths between 5 and 15 m, two fresh water discharge q= 1 and 5 m^2/s and different longitudianl density gradients (dg) between 0.0005 and 0.01 kg/m^3/m derived from **Figure 4**. It is noted that the dg-parameter is strongly related to the water depth. A larger water depth means a longer salinity intrusion and hence a smaller dg-parameter, see **Figure 4**. Measured residual velocities are available (**Figure 5**) for spring tide (10 September 1975) with a river discharge of 3 m^2/s per unit width and a water depth of about 15 m near Hoek van Holland at about 4 km from the Sea (Deltares 1984; Van Rijn 2011). Measured residual velocities are in the range of 0.25 to 0.35 m/s near the bottom and in the range of 0.35 to 0.45 near the water surface. The computed velocities show reasonable agreement with the measured data for γ=0.003 (calibration parameter related to mixing coefficient, Part I). The computed circulation velocities increase with increasing river discharges and with increasing water depths. The overall effect of water depth is rather small, but the effect of increasing river discharge is very pronounced as the stratification effect is enhanced. An increase of the river discharge from 1 to 5 m^2/s at a water depth of 5 m results in an increase of the near-bed peak velocity of about 20%. A similar increase of the river discharge at a water depth of 15 m results in a velocity increase of 50%.


Figure 5 *Effect of water depth and river discharge on residual velocity profiles due to longitudinal density gradients (dg) for prismatic channel (Peak tidal velocity= 1 m/s; Bed roughness =0.01 m)*

Based on these results, we conclude that the near-bed residual velocities increase very weakly for increasing water depths. We found that the near-bed peak residual velocity is roughly proportional to $u_{rs} \sim h_o^{0.1}$ for a low discharge and $u_{rs} \sim h_o^{0.3}$ for a high discharge. The main reason for this weak effect of near-bed velocity on water depth is that the density gradient, which was determined from the salinity model of Kuijper van Van Rijn (2011) applied to a prismatic channel, strongly decreases for increasing water depth (see **Figure 4**).

The present model produces similar results as the methods of Hansen and Rattray (1965), Chatwin (1976) and Talke et al. (2009). Their models have a maximum value at about 0.25h and show increasing residual velocities for increasing water depth and increasing river discharge.

We should note here that the simplified model of the vertical distribution of the residual velocities can only represent basic circulation features. The maximum landward velocity always is at about 0.25 h and continuity is preserved locally (equality of landward and seaward flow). A realistic pattern of the residual velocities along the prismatic channel of the Rotterdam Waterway can be obtained from 3D-model computations for three fresh water river discharges (5%, 50% and 95% river discharge at the upstream boundary, German border), see **Figure 6**. The density-driven flow near the bed is largest for springtide in combination with a low fresh water discharge ($Q_{5\%}$) and smallest for neap tide with high fresh water discharge ($Q_{95\%}$). The residual flow velocities in the upper part of the water column are up to 1 m/s near the mouth in seaward direction during neap tide. Near the bed the landward residual velocities are rather constant with values up to 0.25 m/s in the region between km 1030 and 1020 (mouth= km 1035). Measured values at km 1030 are in the range of 0.25 to 0.35 m/s. During springtide, the thickness of the near-bed layer with residual flow in landward direction increases to about 40% of the depth in the region km 1030 to 1020. The residual velocities gradually die out near the head of the salt wedge (km 1010-1005) which has a length scale of about 25 to 30 km during springtide and about 15 km during neap tide.

The results of the 3D-model confirm that the values based on the simplified expression for residual velocities (based on Equation 9 of part I) are of the right order of magnitude and that the calibration coefficient $\gamma=0.003$ is representative for the Rotterdam Waterway. More verification is required to test the validity of the simplified expression for a wider range of conditions.
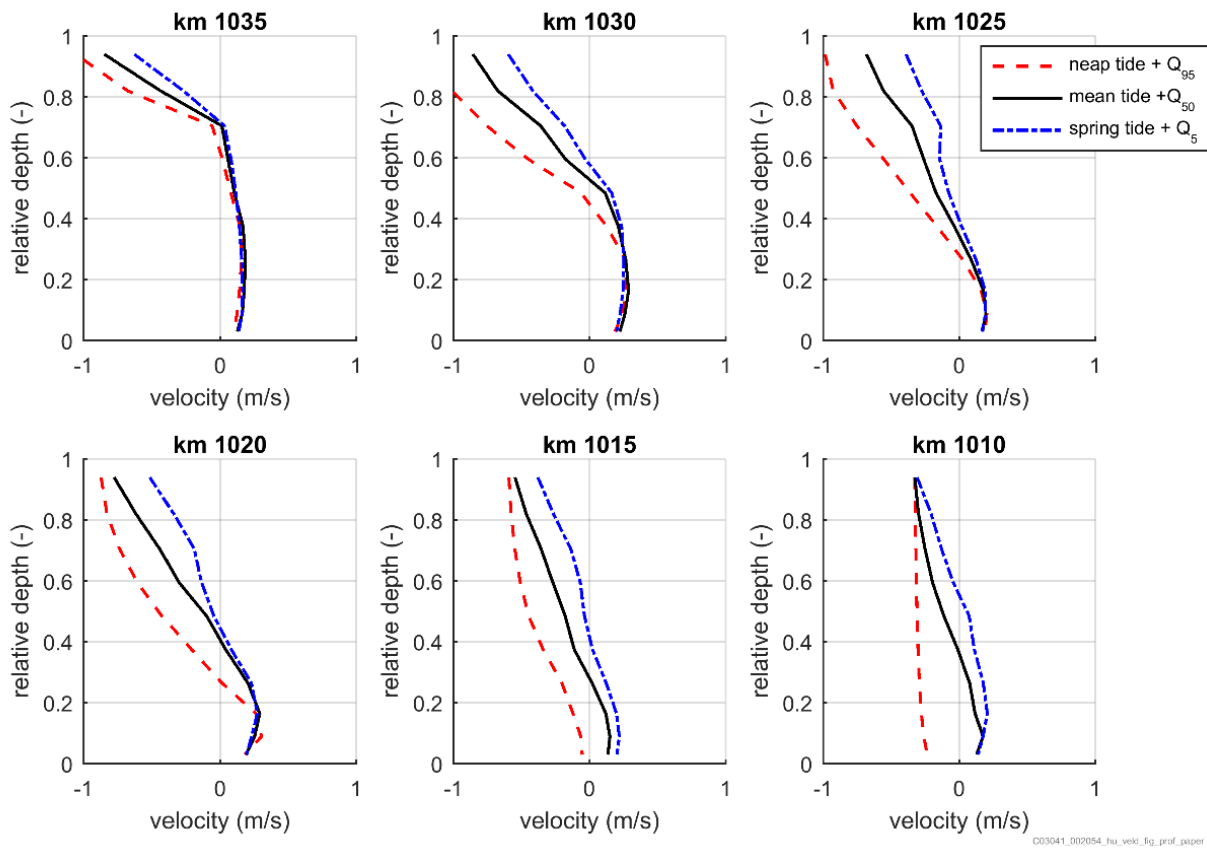
Figure 6   *Computed residual velocities along Rotterdam Waterway based on 3D-model; 1035 km= mouth; tidal range= 1.85 m; river discharges Waterway: Q_5=485 m^3/s, Q_{50}= 1310 m^3/s, Q_{95}=2500 m^3/s (Arcadis 2015)*

3.3 Simplified mud transport

Definitions
The TMUD model describes the mud concentrations and transports over a mud bed in saturated conditions (percentage of mud in the bed > 70%; see Section 1). A sediment bed generally has cohesive properties if the mud fraction (<63 μm) is larger than about 30% (Van Ledden et al. 2004; Van Rijn, 1993, 2007). The hydrodynamics of the TMUD-model are described in Part I. The velocities and concentrations are computed as a function of z and t; z=height above bed and t=time. The grid points over the depth (50 points) are distributed exponentially as follows: $z=a[h/a]^{(k-1)/(N-1)}$ with: a= reference height above bed (input value), $h=h_o+\eta=$ water depth, $h_o=$ depth between bed and mean sea level, $\eta=$ tidal water level, k= index number of point k, N= total number of grid points. Used as standalone model, the basic hydrodynamic parameters should be specified by the user. Used as post-processing model, the hydrodynamic input may come from a 1D, 2DH or 3D-model. TMUD can be used for prismatic and converging channels.

Mud concentrations and transport
Various researchers have shown that the transport of mud over a soft muddy bed can be described by using a saturation or capacity approach (Bagnold, 1952; Xu, 1999a,b; Winterwerp, 2001, 2006, 2011; Van Rijn 2007, 2015). Winterwerp (2001, 2006) shows that the sediment concentrations near the bed cannot be larger than a maximum value (saturation value) due to the reduction of vertical turbulent velocities by sediment-related stratification effects (turbulence collapse). It is assumed that the saturated mud concentrations are quickly adjusting to the local flow conditions (no significant under or overloading). The saturation concentration (c_{mud}) is found to be proportional to the local velocity U to the power 3 and inversely proportional to the settling velocity (w_{mud}) and water depth (h). Thus: $c_{mud} \sim U^3/(w_{mud} h)$.

Measured saturated depth-averaged concentrations of mud and silt are shown in **Figure 7** for various field locations with tidal and river flow over a muddy/silty bed. We have estimated the depth-averaged concentrations from concentration profile data available in the literature or from the ratio q_s/q with $q_s=$ depth-integrated transport rate and q= water discharge rate. The mud concentrations are somewhat larger (factor 2 to 3) than the silt concentrations. Mud concentrations in very large water depths are smaller than mud concentrations in smaller depths at the same depth-averaged velocity, because the bed-shear stresses are smaller for larger depths at the same flow velocity. The mud concentration data strongly depends on the depth-mean velocity and can be represented by $c_{mud}=\alpha U^3/(w_{mud} h)$.
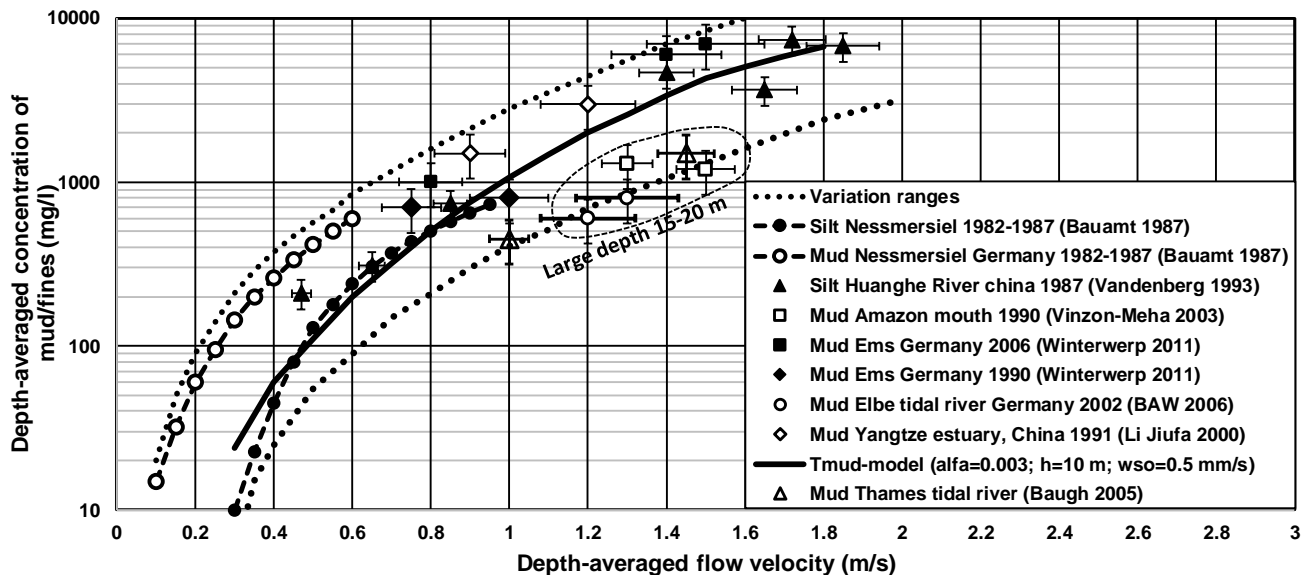
Figure 7 *Depth-averaged mud and silt concentrations as function of depth-averaged flow velocity from various field sites*

The mud concentration profile in saturated conditions can be described by the vertical advection-diffusion equation (Rouse 1938; Van Rijn 1984, 1993, 2007):

$$c \, w_{mud} + \varepsilon_s \, dc/dz = 0 \qquad (1)$$

with: c= volumetric concentration, w_{mud}=settling velocity of mud, ε_s= mixing coefficient. The bed-boundary condition is given by a near-bed concentration (reference concentration; Equation 11 of Part I), which is an empirical function of the excess bed-shear stress (τ_b-$\tau_{cr,e}$) and a calibration factor (Part I). This empirical function is only valid for saturated mud transport conditions. The critical bed-shear stress for erosion of mud is an input value to deal with site-specific conditions (no general relationship is available).

The concentration-dependent mud settling velocity is represented by an empirical equation, as (Van Rijn 2007):

$$w_{mud} = \exp[\alpha_1 \ln(c) + \alpha_2 - \alpha_3]; \qquad \text{for flocculation range } c \leq 0.0025 \qquad (2a)$$
$$\alpha_1 = 0.18 \ln(w_{mud,max}/w_{mud,min})$$
$$\alpha_2 = 2.1 \ln(w_{mud,max})$$
$$\alpha_3 = 1.1 \ln(w_{mud,min})$$
$$w_{mud} = w_{mud,max}(1-c)^4 \qquad \text{for hindered settling range } c > 0.0025 \qquad (2b)$$

with: $w_{mud,max}$= maximum settling velocity at volumetric concentration c=0.0025 ($w_{mud,max} \cong 2$ mm/s; input value), $w_{mud,min}$=minimum settling velocity at c=0.00001 ($w_{mud,min}$=0.5 mm/s; input value). Both parameters define the range of the settling velocity due to flocculation effects. Details of the flocculation and hindered settling effects are given by Van Rijn (2007).

The sediment mixing coefficient (eddy viscosity) distribution in the presence of high concentrations in the lower part of the water column is represented by a linear semi-analytical distribution related to bed-shear velocity, as follows:

$$\varepsilon_s = \phi_d \, \varepsilon_b \qquad \text{for } z \leq \delta_{fm} \qquad (3a)$$
$$\varepsilon_s = \phi_d \, [\varepsilon_b + (\varepsilon_{max} - \varepsilon_b)(z-\delta_{fm})/(0.5h-\delta_{fm})] \qquad \text{for } \delta_{fm} < z < 0.5h \qquad (3b)$$
$$\varepsilon_s = \phi_d \, [(h-z)/(0.5h)] \, \varepsilon_{max} \qquad \text{for } z \geq 0.5h \qquad (3c)$$
$$\varepsilon_{max} = 0.05 \, u_* \, h$$
$$\varepsilon_b = 0.5 \, \varepsilon_{max}$$

with: δ_{fm} = thickness of fluid mud layer (input value), ε_b= sediment mixing coefficient in fluid mud layer, ε_{max}= maximum sediment mixing coefficient at z/h=0.5, h= water depth, u_*= bed-shear velocity, ϕ_d= turbulence damping coefficient (function of Richardson number Ri), Ri= $[-(g/\rho)][d\rho/dz]/[(du/dz)^2]$= $[-(\rho_s-\rho_w)g/((\rho_w+(\rho_s-\rho_w)c))][dc/dz]/[(du/dz)^2]$, ρ= fluid-sediment mixture density=$\rho_s c+(1-c)\rho_w$, c= volumetric concentration.

The damping function related to stratification effects is expressed as (Munk and Anderson 1948):

$$\phi_d = (1 + \alpha_d \, 2Ri^{0.5})^{-1} \qquad (4)$$

with: α_d= calibration coefficient (default=1; in range of 0 to 2).
Equation (1) for mud concentrations is solved by numerical integration to include the turbulence damping effect. Neglecting this effect, an analytical solution is possible.

3.4 Model validation

The range of measured mud concentrations (field data) of **Figure 7** has been used for model calibration assuming a channel depth of 10 m with depth-mean velocities between 0.3 and 1.8 m/s and a mud settling velocity of 0.5 mm/s. The mud concentration data of **Figure 7** can be represented for a calibration coefficient α= 0.003 (±factor 3) of the near-bed concentration function. Default values were used for all other coefficients (see Van Rijn, 2007). Both the measured and computed data show that the depth-averaged concentration of fine sediments (<63 μm) vary systematically with the depth-mean velocity in saturated flow conditions (confirming the saturation theory). The measured values represent a very wide range of conditions with flow velocities between 0.3 and 1.8 m/s at many different sites. Given the relatively large variation range of **Figure 7**, the calibration factor α=0.003 only gives an order of magnitude estimate for arbitrary sites. Additional calibration based on field data from each specific site should always be done.

To validate the vertical distribution of the computed mud concentrations, we have used measured mud concentration profiles from the Amazon River in Brasil (Vinzon and Mehta 2003). The mud concentrations were measured at a sheltered location in the lee of Cabo Norte shoal. The mean depth at the site was about 16 to 18 m. The spring tidal range was about 3.1 m. Current

velocity profiles were measured with an electromagnetic current meter and suspended sediment concentrations with an optical backscatter instrument (OBS). The lowest measurement elevation was 0.25 m above the level at which the profiler rested on the bed.

Measured and computed mud concentrations over the water depth at maximum tidal flow in the mouth of the Amazon River in Brasil are shown in **Figure 8**. Computed concentrations are based on the following input values: water depth h= 17 m, tidal range= 3 m, U_{max}= 1.35 m/s, T= 45000 s, salinity gradient $d\rho/dx$= 0, settling velocity $w_{mud,max}$= 0.002 m/s, $w_{mud,min}$= 0.0005 m/s, grain roughness = 0.0001 m, velocity profile roughness = 0.1 m, ρ_s= 2650 kg/m^3, ρ_w= 1025 kg/m^3, ν= 0.000001 m^2/s, $\tau_{b,cr,mud}$= 0.1 N/m^2, thickness fluid mud layer δ_{fm}= 2 m, α_d= 1 (Ri-approach for damping function). Our main aim was in this case to validate the vertical distribution of the mud concentrations. Therefore, the measured bed concentration at the lowest measurement level (0.25 m above bed) was used as bed boundary condition. A constant settling velocity of 2 mm/s yields the best agreement with measured concentrations. A concentration dependent settling velocity between 0.5 and 2 mm/s yields higher concentrations in the upper part of the water column due to smaller settling velocities. The inclusion of damping of turbulence due to sediment stratification effects appears to be essential for this case. Neglecting this effect, the computed concentration profile was much more uniform over the depth (large overprediction). This type of effect can only be included by numerical integration. Analytical models cannot represent this effect with sufficient detail.

To validate the tidal variation of the mud concentrations and the tide-integrated mud transport of the standalone TMUD-model, we have used measured field data from the mouth region of the Ems River (Station Leer; water depth to MSL= 7 m; effective channel width= 200 m), based on the data of Winterwerp (2011). The original data were measured by Van Leussen (pages 330 to 350, 1994), who measured current velocities and mud concentrations (optical sensor+ water samples for calibration) at 0.3, 0.5, 1, 2 and 4 m above the bed and 1.5 m below the water surface at each hour during the tidal cycle. Based on these detailed measurements, the depth-integrated mud transport (error < 30%) was estimated by Van Leussen. The tidal range is about 2.8 m (mean tide). The peak tidal flood velocity is about 1 m/s and the peak ebb velocity is about 0.8 m/s. The phase shift between the horizontal and vertical tide is about 3 hours. The specific river discharge per unit width is quite low (0.1 m^2/s). It is assumed that the horizontal salinity-gradient can be neglected. The calibration coefficient of the near-bed concentration function is set to α=0.003 (default value; no additional calibration). The computed depth-integrated mud transport is shown in **Figure 9**. The computed transport values are in reasonable agreement with the measured data but the timing is less well predicted. The latter is caused by the application of a sinusoidal tidal velocity in the model. The measured tidal velocity shows a pronounced asymmetry with time, which cannot be represented with sufficient accuracy by the standalone TMUD-model. The computed net tide-integrated mud transport is about 13 ton/m/tide (37 ton/m/tide for flood and 24 ton/m/tide for ebb). The measured net tide-integrated mud transport is 8.5 ton/m/tide (slightly larger than the range given in **Table 1**).

Based on these comparisons, we can conclude that the simplified mud model TMUD produces mud concentration profiles and mud transport rates of the right order of magnitude in saturated mud conditions (mud percentage in bed > 70%) if sufficient input data are available. We emphasize here that TMUD is a local model (neglecting horizontal gradients as present in the ETM). The model is not valid for non-saturated (supply limited) conditions (Section 1). However, the TMUD-model yields surprisingly good results for the Elbe River with non-saturated mud transport (percentage of mud in bed of about 35%) if the percentage of mud in the sandy bed is properly taken into account (**Section 5**).
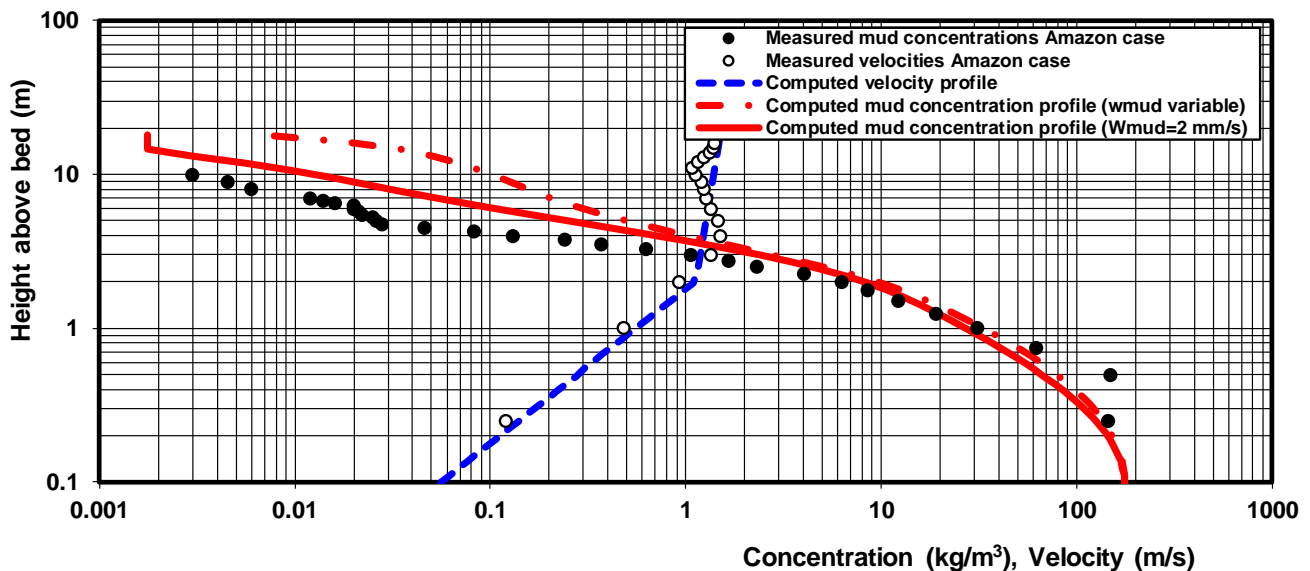
Figure 8   *Measured and computed mud concentration profiles in the mouth of the Amazon, Brasil; TMUD-model results*
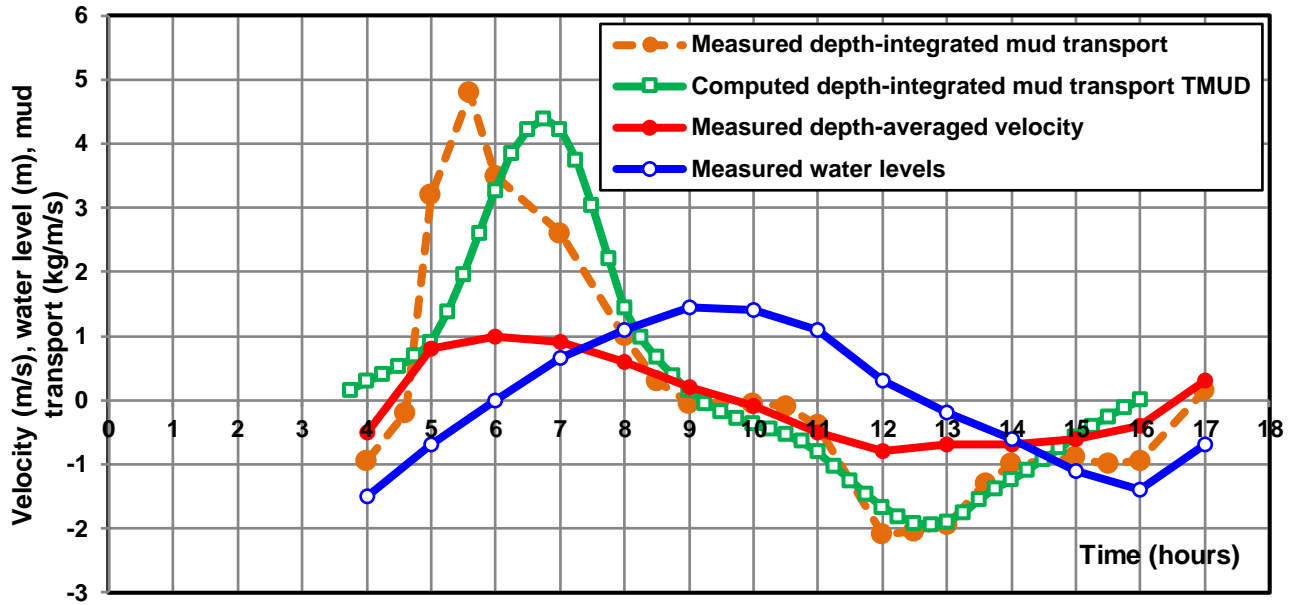
Figure 9   *Tidal variation of measured and computed velocity, water levels, depth-integrated mud transport, Ems river near Leer; TMUD-model results (data given by Winterwerp 2011; original data from Van Leussen 1994)*

4.   Effect of channel deepening on tide-integrated mud transport along Rotterdam Waterway; 3D-model

To gain a better understanding of non-saturated mud transport processes and ETM-generation in the prismatic Rotterdam Waterway, we performed some exploring runs using the Delft3D-model for the neap-spring tidal cycle. The 3D-model includes salinity driven flows, see **Figure 6**. The Rotterdam Waterway (see Section 2) has a dominantly sandy bed with relatively small mud percentages of 5% to 35% (non-saturated mud transport). The 3D-model includes most relevant processes: horizontal and vertical advection and diffusion, turbulence damping effects due to sediments, flocculation effects on the settling velocity of mud (Equation 2a), hindered settling effects (Equation 2b). Turbulence modelling is done by the K-epsilon equations (production and decay of turbulence energy). The bed boundary condition is prescribed by a near-bed concentration function, which is also used in the simplified model (Part I).

The model domain extends from the seaward boundary at the 20 m depth contour up to the river boundary at a depth of 5 m far upstream. A constant significant wave height of 1.5 m and wave period of $T_p = 8$ s was applied at sea to stir up mud from the seabed. The model bed consisted of a top layer with thickness δ and bulk density $\rho_{mixture}$ consisting of sand and mud (silt/clay). The layer thickness δ, the bulk density and the masses of sand and mud of the top layer are related by: $M_{mud} + M_{sand} = \delta \rho_{mixture}$. (for example: $\delta = 0.1$ m, $\rho_{mixture} = 1250$ kg/m^3 and prescribed initial value $M_{mud} = 50$ kg/m^2 yields computed initial value $M_{sand} = 75$ kg/m^2). If M_{sand} and M_{mud} are changing as function of time, the bulk density of the top layer of 0.1 m is recomputed. The thickness of top layer remains constant and moves with the bed surface up and down depending on deposition and erosion values. The bed composition of the sandy channel bed with varying percentages of mud along the channel is schematized in agreement with observations (about 5% mud at km 1035 gradually increasing to 10% up to km 1015 and up to 35% at km 1010). The mud is represented as sediment with $d_{50} = 20$ μm and can be picked up from the bed in the mouth region in proportion to the availability. The flocculation effect in Delft3D is taken into account by Equation (2a).

The model with sea waves included was calibrated by adjusting A) the mud concentration at the river boundary in the range of 20 to 40 mg/l and B) the mud concentration at the sea boundary in the range of 15 to 30 mg/l. The model runs were repeated until the tide-integrated mud input at the mouth km 1035 was about 4 ton/m/tide (import) over the neap-spring cycle, which is of the right order of magnitude (see **Table 1**).

The model is capable of simulating the tide-averaged (spring-neap cycle) mud concentrations near the bed and near the water surface along the Rotterdam Waterway, as shown in **Figure 10**. The computations show a turbidity zone (ETM) with near-bed mud concentrations of about 100 mg/l and near-surface concentrations of 10 to 20 mg/l in the section between km 1025 and km 1015. The computed concentration values are somewhat smaller (factor 2) than the observed values (**Figure 2**). We should note here that the model run is not a direct simulation of the observation results of De Nijs (2012) but rather an

15

exploring run for similar conditions. The measured mud concentrations of **Figure 2** (based on the field data of De Nijs 2012) refer to springtide with a fresh water discharge of about 1700 m^3/s, whereas the model results are based on the mean tide and a river discharge of 1310 m^3/s. This may explain why the computed concentrations are smaller (factor of 2) than the measured values.

The computed mud import from marine sources is about 4 ton/m/tide for situations with relatively low waves just outside the mouth. Without waves at sea, the mud concentrations of the ETM are smaller (factor 2; not shown). This stresses the importance of waves as mud stirring mechanism. More research into the effect of waves on the stirring of mud outside the mouth region on the generation (by advection process) of ETM is required to evaluate the effect of extreme events with storms. The computed upstream fluvial mud input per unit width is about 4 ton/m/tide. The annual-mean import in the mouth region also is about 4 ton/m/tide, which means that the computed mud input from fluvial and marine sources are of the same order of magnitude.

Annually, the total mud input in the ETM zone is about (4+4) x 730 (number of tides) x 500 (width) = 3 million ton/year or about 7.5 million m^3/year assuming a dry bulk density of 0.4 ton/m^3. This value is of the same order of magnitude as the annual dredging volume of mud of about 9 million m^3/year (mostly from the harbour basins/entrances where soft mud accumulates). This order of magnitude analysis shows that the model results are realistic and can be used for engineering studies.
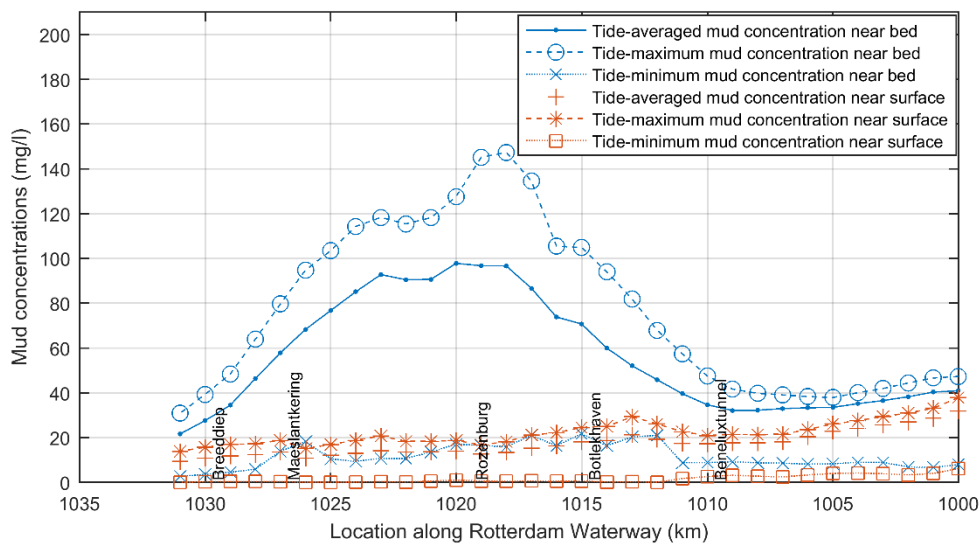
Figure 10   *Computed mud concentrations in ETM of Rotterdam Waterway (present situation); neap-spring tidal cycle and $Q_{waterway,50\%} = 1310\ m^3/s$; North Sea at km 1035; Delft3D-model (Arcadis 2015)*
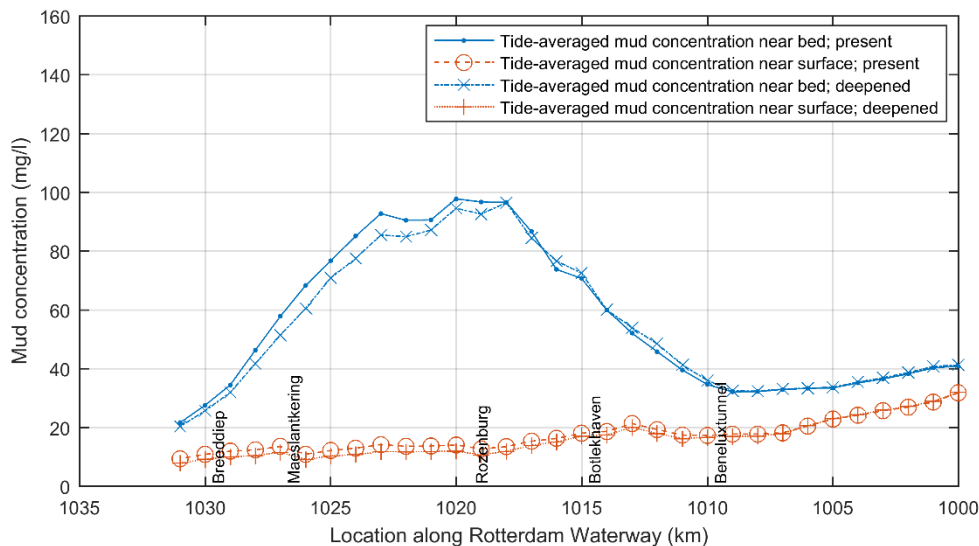
Figure 11   *Computed mud concentrations in ETM; present and deepened channel of Rotterdam Waterway; neap-spring tidal cycle and $Q_{waterway,50\%} = 1310\ m^3/s$; North Sea at km 1035; Delft3D-model (Arcadis 2015)*

Hereafter, the effect of channel deepening (from 15 m to 16.3 m between km 1010 and 1030) on the mud concentrations along the Rotterdam Waterway is discussed. **Figure 11** shows the computed tide-averaged mud concentrations in the present channel and in the deepened channel. The near-bed mud concentrations are slightly smaller (5% to 10%) in the mouth section between km 1030 and 1020 and slightly larger (5% to 10%) in the section km 1020 and 1010, which is the effect of the increased landward shift of the salt wedge. However, the increase of the deposition of mud in the landward sections km 1015 to 1005 is computed to be significantly larger (about 30%) due to lower near-bed flood velocities in the deepened sections (see Part I). Furthermore, the deposition of mud in the inland docks in these sections was computed increase by about 20% due to the higher mud concentrations and increased trapping (increased salinity), (Arcadis 2015). In addition to the higher mud concentration in the ETM, the density-driven inflow near the bed at the dock entrance will increase due to the presence of a larger water depth (10%) at the dock entrance and a slightly larger tidal range. An important effect is the landward shift of the ETM, which will change the phasing between the maximum mud concentrations and the maximum salinity in front of the dock entrances. Hence, certain docks may get less deposition whereas other docks may get more deposition.

Overall, it is concluded that the non-saturated transport of mud over a sand bed (mud percentages of 5% to 35%) along the Rotterdam Waterway can be represented to some extent by the 3D-model when sea waves are included to stir up mud from the seabed. The mud concentrations in the ETM are supplied by mud from the upstream river flow and by mud from marine sources. The supply of river mud and the trapping of river mud by the salt wedge will not change after deepening of the navigation channel. However, the density-driven near-bed velocities during flood tide will increase carrying more mud to the salinity head which is further inland (increase of salinity penetration).

5. Effect of channel deepening on net mud transport at mouth of tidal channels; standalone TMUD-model

To get a better understanding of the export and import of mud in the mouth region of a stratified tidal system and the conditions of regime shift from export to import for a wide range of river discharge and water depths, we applied the TMUD-model as a standalone model for saturated mud flow conditions in a prismatic tidal channel (like the Rotterdam Waterway). The model computes the velocity and concentration profiles over the tidal cycle at a fixed location in the mouth region of a tidal channel. Tidal integration yields the net tide-integrated transport rates. Gravitational circulation effects due to longitudinal density gradients are taken into account. Horizontal advection and diffusion are not taken into account.
The range of flow and salinity conditions is exactly the same as those used in Section 4.2 of Part I. The tidal channel is assumed to have a mud bed consisting of 70% mud and 30% fine sand ($p_{mud}= 0.7$ and $p_{sand}= 0.3$) and water depths in the range of 5 to 20 m. The settling velocity is concentration-dependent with settling velocities between 0.5 and 2 mm/s representing the effects of flocculation and hindered settling. The calibration factor of the near-bed concentration is set to the default value of $\alpha=0.003$ which yields mud concentrations near the bed in the range of 1 to 10 kg/m^3. Other input values are: tidal range H= 2 m, sediment roughness of $k_s= 0.0001$ m for mud entrainment and $k_s=0.1$ m for the velocity profile, critical bed-shear stress of mud $\tau_{cr,mud}= 0.3$ N/m^2 (equivalent to critical depth-averaged velocity of about 0.35 m/s) The horizontal salinity gradients are prescribed based on the values given in Part I (representative for a prismatic tidal channel as the Rotterdam Waterway). The most uncertain input parameters are the tidal velocity asymmetry and the horizontal density gradients.

The focus point of this section is the value of the computed net tide-integrated mud transport at a fixed location in a tidal channel with saturated mud flow conditions as function of the water depth and the river discharge, see **Figure 12**. The computed results should be seen as order of magnitude estimates with a variation range of a factor of 2 due to uncertainties involved (tidal asymmetry, salinity gradients; mud erosion function).
The net tide-integrated mud transport rate clearly decreases for increasing water depth, particularly for depths in the range of 5 to 15 m, which is mainly caused by decreasing bed-shear stresses and mixing properties for increasing water depth (as discussed in Part I). Thus, the exporting/flushing capacity of the tidal channel decreases with increasing channel depth. The river discharge at which there is a shift from export to import of mud gradually increases from $q_r= 1$ m^2/s for h= 5 m to $q_r= 3.5$ m^2/s for h=20 m. In the case of a relatively large depth (> 10 m), flushing conditions (export) require a relatively large river discharge (as found by Talke et al., 2009; Winterwerp 2011, Winterwerp et al. 2013). At shallow depth (< 5 m), export of mud is present most of the time. Mud import at a depth of 5 m only occurs for a very small river discharge < 1 m^2/s. At very low river discharges (< 1 m^2/s) the net mud import is almost constant (about 10 to 20 ton/m/tide) for water depths between 5 and 20 m. The mud concentrations are relatively uniform over the depth and decrease slightly for increasing water depth as the bed-shear stress decreases for increasing depth at the same velocity. This reduces the depth-integrated mud transport, but it is partly compensated by the larger integration (water) depth.
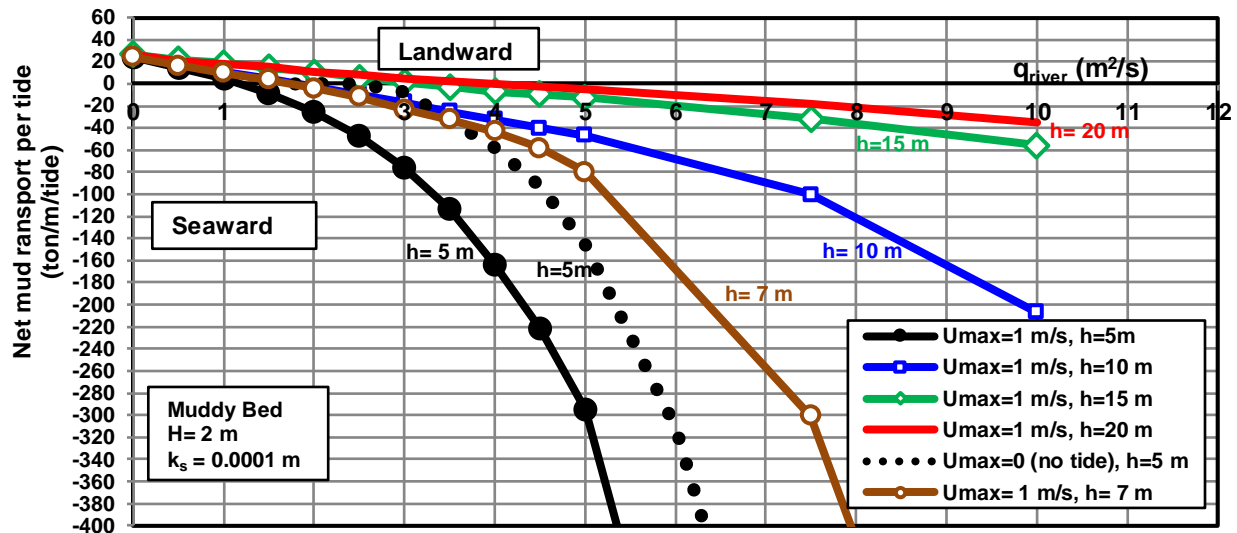
Figure 12 *Effect of water depth and river discharge on net tide-integrated mud transport at a fixed location in the mouth region of a prismatic channel with saturated mud flow; TMUD-model results*

The consequences of the results of **Figure 12** can be best explained by taking a prismatic tidal channel as an example. For this purpose we consider two fixed locations: upstream river section (no tide) and downstream tidal mouth region, both with an equal water depth of 5 m. The upstream mud transport for a depth of 5 m and a river discharge of 4.5 m^2/s (river velocity of 0.9 m/s; Rhine River) is about 100 ton/m/tide (export to the sea). The mud export in the tidal mouth region at a depth of 5 m and at the same river discharge of 4.5 m^2/s is about 220 ton/m/tide. Thus, the section between the upstream river location and the tidal location will erode until the net tide-integrated mud transport in the mouth region is 100 ton/m/tide, which will occur for a depth of 6 to 7 m at the tidal location (**Figure 12**). For depths larger than 7 m, the net tide-integrated transport is smaller than 100 ton/m/tide (for example 40 ton/m/tide for h= 10 m) resulting in deposition in the section between both locations. The depth of 6 to 7 m at the tidal location can be seen as the 'equilibrium' depth at that location in the mouth region. Thus, the shift from erosion to deposition occurs at a depth of about 6 to 7 m in the case of a muddy bed. It is noted that for sandy beds (Part I), the shift from erosion to deposition occurs at a depth of 9 to 10 m. If the channel banks are erodible (no dikes or groins), both the width and depth of the channel will adjust to form a converging tidal channel. Most likely, the 'equilibrium' depth in the mouth region of weakly converging channels will be similar to that in a prismatic channel, as the peak tidal velocities in the mouth region are similar (Part I).

If the bed of the tidal channel consists of soft mud with saturated mud flow and the river discharge is relatively large, the net tide-integrated transport rate of mud is seaward (export). In the case of deepening of a prismatic or weakly converging channel, the peak tidal velocities in the mouth region will, most likely, remain more or less constant (Part I). However, the salinity intrusion and near-bed density-driven flow in combination with the tidal flood current will increase and the salinity head will shift in landward direction over a distance of 5 to 10 km due to the deepening effect. Similarly, the ETM will shift landward while the mud concentrations in the ETM may increase slightly due to the increase of the density-driven flow. Deepening of the tidal channel will lead to less river flushing capacity and thus a reduction of the export capacity, particularly for depths increasing from 5 to 15 m, as found by others (Talke et al. 2009). For relatively low river discharges ($q_r < 1$ m^2/s) the net tide-integrated mud transport is in landward direction (import). Deepening of an already deep channel from 15 to 20 m does not lead to a significant increase (less than 10% to 15%) of the net mud import rate and deposition volume. The net mud import remains at a relatively high value of about 10 to 20 ton/m/tide (**Figure 12**). The effect of further deepening on deposition is small and thus further deepening may be attractive for economic reasons.

However, conditions with low discharges, large depths and large salinity intrusion are very favourable for the formation of fluid mud layers (not represented in the TMUD-model), especially around neap tides in a stratified system. Fluid mud can also form at HW and LW slack tides (Schrottke et al., 2006). The relatively high concentrations in the lower part of the water column near the head of the salinity wedge (ETM) will have more time for settling and fluid mud formation during neap tide due to the presence of relatively low velocities. Fluid mud with a smooth surface will reduce the flow resistance resulting in larger tidal penetration and salinity intrusion. The asymmetry of velocity and mixing over the tidal cycle may increase resulting in more import of mud (tidal pumping; positive feedback). This may all lead to a substantial increase of the mud import in the case of fluid mud formation. At low river discharges, fine sediments can be transported beyond the head of the

18

salinity wedge if the peak flood velocities are somewhat larger than the peak ebb velocities (velocity asymmetry), particularly when fine sediments are abundantly present in the upstream river bed. In this regime, a relatively large region of turbid water will be present moving landward and seaward with the tide. The length of this region will increase for increasing water depth. Harbour docks landward of the turbidity zone will have more mud deposition as the higher mud concentrations of the flood currents will enter the docks. The Hamburg port docks along the tidal Elbe River show this behavior (see Section 2).

The mud deposits associated with the turbidity maximum can only be flushed out of the tidal channel in conditions with large river discharges ($q_r > 5$ m^2/s; $\overline{u}_r/\overline{U}_{max} > 0.5$). Hereafter, the results of **Figure 12** are compared to the measured values (**Table 1**) of the tidal systems of the Ems, Elbe and Rotterdam Waterway

In this way the presence of fluid mud may lead to significant more import of mud. It is noted that model approach used (TMUD-model) is not valid for conditions with fluid mud.

Tidal Ems River: The present results show that, at low river discharges ($q_r < 0.5$ m^2/s), the system can be gradually loaded with mud from the outer estuary/sea which can only be flushed out sufficiently at relatively large river discharges ($q_r > 3$ m^2/s), as observed in the Ems River, Germany. **Figure 12** yields a net tide-integrated mud import of about 10 ton/m/tide for the Ems River with a unit river discharge of about 0.3 m^2/s and a water depth of 7 to 8 m. This predicted value of 10 ton/m/tide is about twice as large as the values given in **Table 1**, which is a very reasonable result for a mud model prediction.

Tidal Elbe River: Using the data of the Elbe River (**Table 1**) with a water depth of 15 m; unit river discharge of 0.5 m^2/s, the net import of mud in the mouth region of the Elbe is about 15 ton/m/tide (**Figure 12** for saturated mud flow), which is much larger (factor 2 to 3) than the estimated import values given in **Table 1**. The overprediction can be related to the presence of non-saturated mud flow as the bed of the Elbe consists of sand and mud (along-channel average of about 35% mud; BAW 2006). The prediction can be improved by multiplying the net tide-integrated transport for saturated mud flow with the percentage of mud present in the bed yielding a value of $0.35 \times 15 \cong 5$ ton/m/tide.

Rotterdam Waterway: Using the data of the Rotterdam Waterway (**Table 1**) with a water depth of 15 m and a river discharge of about 2.5 m^2/s, the computed net import of mud is about 10 ton/m/tide (**Figure 12**), which is significantly larger (factor 1.5) than the estimated import values of about 6 ton/m/tide from dredging records given in **Table 1**. **Figure 12** is however valid for saturated mud transport, whereas the Rotterdam Waterway represents non-saturated mud flow over a sandy bed with variable mud percentages between 5% and 35% resulting in lower net tide-integrated transport rates. Furthermore, sea waves are present in the mouth region of the Rotterdam Waterway in the winter season resulting in a larger import of mud due to wave stirring of mud from the seabed into the water column just outside the mouth (Winterwerp and Van Kessel 2003). The effect of seawaves is, however, not (yet) included in **Figure 12**. More research on mud transport in non-saturated conditions and mud erosion from the seabed by waves is required to better deal with these processes.

6. Discussion and conclusions

In this paper we identified and discussed the basic processes influencing the transport of mud in tidal channels (Ems, Elbe and Rotterdam Waterway) with different regimes. We applied detailed and simplified models of tide- and density-driven currents, mud transport and verified these with various field data sets of current velocities and mud transport.

The application of the detailed Delft3D-model for the Rotterdam Waterway shows that the model can simulate mud flow over a sandy bed, provided that sea waves are taken into account to stir up mud from the seabed.

The simplified TMUD-model can be used to estimate the mud transport in saturated mud flow conditions as present in the mouth region of the Ems River for example. Information on salinity and sediment composition should be available for the model to be used as standalone model. In particular, the horizontal salinity variations (gradients) and the percentage of mud present along the bed and banks should be known. The TMUD-model overpredicts the mud transport rates for non-saturated mud flow over a mixed sand-mud bed such as in the Elbe River and the Rotterdam Waterway. The percentage of mud in the bed should be taken into account here. However, it is not yet precisely known how to do this, but will be addressed in future research.

The transport of mud at low fresh water discharges is somewhat different from the transport of sand at low discharges (Part I). The net import of sand shows a marked decrease (from 5 to 1 ton/m/tide) for increasing water depth at low river discharges, whereas the import of mud shows an increase (from about 5 to 20 ton/m/tide) for increasing depth. The sand concentrations near the bed show a much larger decrease for larger water depth with decreasing bed-shear stresses. The compensation effect of a larger integration (water) depth is small for sand as the sand concentrations in the upper part of the water column are relatively small, whereas these compensation effects are substantial for mud transport with relatively high concentrations in the upper part of the water column.

According to Talke et al. (2009), Chernetsky et al. (2010), Winterwerp (2011), Winterwerp and Wang (2013) and De Jonge et al. (2014), the deepening of tidal channels may result into a regime shift from non-saturated mud flow over a sandy bed to saturated mud flow over a muddy bed including the formation of pronounced ETM, fluid mud and mud deposition due to higher mud concentrations (hyper-concentrated flow conditions) over longer distances.

Based on the present results, this regime shift from export to import of mud may occur if:

- the original bed with non-saturated mud flow is sandy with a relatively rough surface and the bed after deepening becomes muddy with a smooth surface (change in bed roughness);
- the water depth at the mouth is changed (dredged) to a value which is larger than the 'equilibrium' water depth (about 6 to 7 m) so that tidal penetration, salt intrusion and mud deposition is promoted for increasing depth; this value of the equilibrium depth agrees well with the data of the Ems River.
- the fresh water river discharge is relatively low and without large extreme values (minimum river flushing) so that a stratified system with density-driven residual flow is present near the bed promoting net import of mud from marine sources;
- the velocity asymmetry is relatively large (much larger flood velocities than ebb velocities);
- the variation of the tidal range over the neap-spring tidal cycle is relatively large, so that relatively long periods with low velocities around neap are present promoting deposition and fluid mud formation with a smooth surface (larger tidal penetration and salt intrusion; positive feedback).

Further deepening of an already deep channel only has a marginal effect (< 10 to 15%) on the import of mud and thus on dredging rates in the mouth region landward of the ETM. The increased deposition in the salinity head zone (local effect) may be as large as 30% as indicated by the 3D-model results due to the reduction of the near-bed flow velocities in that zone. Given the limited increase of deposition rates, further deepening of an existing deep navigation channel is attractive for economic reasons, but the effects of channel deepening on other processes (salinity levels of nearby farmland, ecology) may be much larger and should be studied properly.

The examples of the tidal Elbe River and the tidal Rotterdam Waterway with mixed sand-mud beds show that the simplified TMUD-model results of **Figure 12** (only valid for saturated mud flow) significantly overestimate (factor 3) the net tide-integrated mud import for non-saturated mud transport conditions. The predicted values can be significantly improved by taking the percentage of mud of the bed into account. This can be done by simply multiplying the net tide-integrated transport of **Figure 12** with the along-channel averaged percentage of mud resulting in quite acceptable results for the Rotterdam Waterway. More research is required to study whether this a meaningful generic approach for non-saturated mud transport. The effect of extreme events (storms) on the import of mud in the mouth region should be much better studied. The application of the Delft3D-model to the Rotterdam Waterway shows that sea waves are required to get a realistic ETM.

A real advantage of the simplified TMUD-model is the rapid assessment of the export or import of mud at locations in the mouth region of a tidal channel for a range of hydrodynamic and sediment conditions including storm events (sensitivity studies). The model can be used to explore the effect of sea waves on the stirring of mud from the bed into the water column. Mud concentrations in the Rotterdam Waterway are generally small in the summer season (< 50 mg/l) and larger (> 100 mg/l) in the winter season. Studies on the effects of storm events on the stirring of mud just outside the mouth region are lacking and should get more attention. The simplified TMUD-model is a powerful tool to analyse measured mud concentration profiles with respect to the most appropriate settling velocity as influenced by flocculation and hindered settling effect. The simplified model can be used to derive an effective settling velocity which yields the vertical distribution of the measured concentration profiles. This effective settling velocity can then be used in 3D-model runs

The most important findings related to channel deepening are:
1. Channel deepening to depths larger than the "equilibrium" depth of 6 to 7 m in saturated mud flow leads to a regime shift from mud export to mud import in saturated mud flow conditions. The equilibrium depth is the depth at which the net tide-integrated mud transport in the mouth region is equal to the mud transport in the steady upstream river flow. The equilibrium depth is about 6 to 7 m for muddy tidal channels and 9 to 10 m for sandy tidal channels (Part I).
2. Further deepening of an already deep channel only leads to a marginal increase of the depth-averaged mud concentrations (< 10% to 15%), but the local deposition rates in the salinity head zone may increase by about 30% due to reduction of the near-bed velocities (based on 3D-model results).
3. Channel deepening has a relatively strong effect on the salinity intrusion ($\sim h_o^{2 \text{ to } 2.3}$); Channel deepening by about 10% leads an increase of about 20% of the salinity intrusion in prismatic channels.
4. Channel deepening has a relatively weak effect on residual velocities related to estuarine circulation ($\sim h_o^{0.1 \text{ to } 0.3}$); channel deepening by about 10% leads to a slight increase of about 3% of the maximum density-driven current velocity in the near-bed region of prismatic channels.
5. A pronounced ETM is generated in tidal channels with a mud bed (percentage mud > 70%; Ems) or a sand bed with sufficient mud (percentage mud 30% to 50%; Elbe); a weak ETM can be generated in non-saturated mud flow over a sandy bed with minor mud (percentage mud <30%; Rotterdam Waterway).

20

6. The behaviour of a weak ETM in non-saturated mud flow can be simulated by a 3D-model with a mixed sand-mud bed including salinity effects and sea waves for mud stirring at sea.
7. The proposed TMUD-model can be used as a standalone model to simulate the local mud transport processes in the mouth region of saturated mud flows in which the depth-averaged mud concentration responds almost immediately to variation of the depth-mean velocity (based on the saturation concept).

References
Amin, M., 1983. On perturbations of harmonic constants in the Thames estuary. Geophysical Journal of the Royal Astronomical Society, 73(3), 587–603.

Arcadis, 2015. MER Channel deepening New Rotterdam Waterway and Botlek area (in Dutch). Report C03041.002054.0100, Amersfoort, The Netherlands

Asselman, N.E.M., 1997. Suspended matter in the River Rhine. Doctoral Thesis, Department of Physical Geography, University of Utrecht, The Netherlands

Bagnold, R.A., 1962. Auto-suspension of transported sediment; turbidity currents. Proc. Royal Society A, No. 1322, London, UK, 315-319

Bauamt fur Kustenschutz, Norden, 1987. Tiefenstabilisierung von Aussentiefs mit Naturuntersuchungen am Nessmersieler Aussentief (in German). Land Niedersachsen, Germany

Baugh, J.V. and Littlewood, M., 2005. Development of a cohesive sediment transport model of the Thames estuary. Proc. 9th Int. Conf. Estuarine and Coastal modeling, Charleston, South Carolina, USA

BAW, Bundes Anstalt für Wasserbau, 2006. Gutachten zur ausbaubedingten Aenderung der morphodynamischen Prozesse (in German), Report H1c, www.fahrrinnenausbau.de

Burchard H. and Baumert H., 1998. The formation of estuarine turbidity maxima due to density effects in the salt wedge. A hydrodynamic process study. Journal of Physical Oceanography, 28, 2, 309-320.

Chatwin, P.C., 1976. Some remarks on the maintenance of the salinity distribution in estuaries. Estuarine and Coastal Marine Science, Vol. 4, 555-566

Chernetsky, A., Schuttelaars, H., Talke, S., 2010. The effect of tidal asymmetry and temporal settling lag on sediment trapping in tidal estuaries. Ocean Dynamics. 60, 1219–1241.

De Jonge, V.N., Schuttelaars, H.M., Van Beusekom, J.E.E., Talke, S.A. and De Swart, H.E., 2014. The influence of channel deepening on estuarine turbidity levels and dynamics, as exemplified by the Ems estuary. Estuarine, Coastal and Shelf Science, Vol. 139, 46-59

Deltares/Delft Hydraulics, 1984. Calibration and verification of water movement and salt intrusion in tidal model Rijnmond (in Dutch), Report M2000-3, Delft, The Netherlands

De Nijs, M.A.J., 2012. On sedimentation processes in a stratified estuarine system. Doctoral Thesis, Department of Civil Engineering, Delft University of Technology, The Netherlands

DiLorenzo J.L., Huang P., Thatcher M.L. and Najarian T.O.. 1993. Dredging impacts on Delaware Estuary tides. Presented at Proceedings of the 3rd International Conference on Estuarine and Coastal Modeling III, 86-104, Oak Brook, Illinois, USA

Dyer, K.R., 1986. Coastal and estuarine sediment dynamics. Wiley

Erkens, G. 2009. Sediment dynamics in the Rhine catchment. Doctoral Thesis, University of Utrecht, Utrecht, The Netherlands

Familkhalili, R. and Talke, S.A. 2016. The effect of channel deepening on tides and storm surge: A case study of Wilmington, NC. Geophysical Research Letters 43,9138-9147

Festa, J.F. and Hansen, D.V., 1978. Turbidity maxima in partially mixed estuaries. Estuarine Coastal Marine Science 7, 347–359

Gatto, M., Van Prooijen, B.C. and Wang, Z.B., 2017. Net sediment transport in tidal basins: quantifying the tidal barotropic mechanisms in a unified framework. Ocean Dynamics, Vol. 67, Issue 67, 1385-1406

Geyer, W. R., 1993. The importance of suppression of turbulence by stratification on the estuarine turbidity maximum. Estuaries, 16, 1, 113-125.

Geyer, W.R., Trowbridge, J.H. and Bowen, M.M., 2000. The dynamics of a partially mixed estuary. Journal of Physical Oceanography, 2035-2048

Groen, P. 1967. On the residual transport of suspended matter by an alternating tidal current. Netherlands Journal Sea Research 3,564–575

Herrling, G. and Niemeyer, H.D., 2008. Comparison of the hydrodynamic regime of 1937 and 2005 in the Ems estuary by applying mathematical modeling. Harbasins report, 30 p.

Herrling, G., Elsebach, J. and Ritzmann, 2014. Evaluation of changes in the tidal regime of the Ems-Dollard and lower Weser estuaries by mathematical modelling. Die Kuste, 81, 353-368

Jay, D.A. and Musiak, J.D., 1994. Particle trapping in estuarine tidal flows. Journal Geophysical Research 99, 445–461

Jay, D.A., Talke, S., Hudson, A. and Twardowski, M., 2015. Estuarine turbidity maxima revisited: instrumental approaches, remote sensing, modeling studies and new directions. Developments in Sedimentology, Vol. 68, 49-109

Hansen, D.V. and Rattray, M., 1965. Gravitational circulation in straits and estuaries. Journal Marine Research 23, 104–122.

Kerner, M., 2007. Effects of deepening the Elbe Estuary on sediment regime and water quality. Estuarine, Coast and Shelf Science, Vol. 75, 492–500.

Kuijper, K. and Van Rijn, L.C., 2011. Analytical and numerical analysis of tides and salinities in estuaries; Part II: salinity distributions in prismatic and convergent tidal channels. Ocean Dynamics, Vol. 61, 1743-1765

Li Jiufa, He Qing, Zhang Lili and Shen Huanting. 2000. Sediment deposition and resuspension in mouth bar area of the Yangtze estuary. China Ocean Engineering, Vol. 14, 339-348

Munk, W.H. and Anderson, E.R., 1948. Notes on a theory of the thermocline. Journal of Marine Research, Vol. 3, 276-295

Postma, H., 1954. Hydrography of the Dutch Wadden Sea. Arch. Neerl. Zool. 10, 405–511

Postma, H.,1961. Transport and accumulation of suspended matter in the Dutch Wadden Sea, The Netherlands. Journal Sea Research, Vol. 1, 148-190

Prandle, D., 1985. On salinity regimes and the vertical structure of residual flows in narrow estuaries. Estuarine, Coastal and Shelf Science, Vol. 20, 615-635

Prandle, D., 2004. Saline intrusion in partially mixed estuaries. Estuarine, Coastal and Shelf Science, Vol. 59, 385-397

Prandle, D., 2009. Esturies. Dynamics, Mixing, Sedimentation and Morphology. Cambridge University Press.

Rijkswaterstaat, 2000. Mud transport in the Maas-Rijn mouth; results of SILTMAN project (in Dutch). Report RIKZ/2000.027, The Hague, The Netherlands

Rouse, H., 1938. Modern conceptions of the mechanics of turbulence. Trans. Am. Soc. Civil Engrs. Vol. 102.

Sanford, L.P. and Halka. J.P., 1993. Assessing the paradigm of mutually exclusive erosion and deposition of mud with examples from upper Chesapeake Bay. Marine Geology, Vol 114, 37-57

Schrottke, K., Becker, M., Bartholoma, A., Flemming, B.W. and Hebbeln, D., 2006. Fluid mud dynamics in the Weser estuary turbidity zone tracked by high-resolution side-scan sonar and parametric sub-bottom profiler. Geo-Marine Letters. DOI 10.1007/s00367-006-0027-1

Simpson, J.H., Brown, J., Matthews, J. and Allen, YG., 1990. Tidal straining, density currents and stirring in the control of estuarine circulation. Estuaries 13, 125-132

Talke S.A., De Swart H.E. and Schuttelaars H.M., 2009. Feedback between residual circulations and sediment distribution in highly turbid estuaries: an analytical model. Continental Shelf Research 29, 119–135. doi:10.1016/j.csr.2007.09.002

Van den Berg, J.H. and Van Gelder, A., 1993. Prediction of suspended bed material transport in flows over silt and very fine sand. Water Resources Research, Vol. 29, No. 5 p. 1393-1404

Van Ledden, M., Van Kesteren, W.G.M. and Winterwerp, J.C., 2004. A conceptual framework for the erosion behaviour of sand-mud mixtures. Continental Shelf Research 24, 1-11

Van Leussen, W., 1994. Estuarine macroflocs; their role in fine-grained sedimen transport. University of Utrecht, Utrecht, the Netherlands

Van Maren, D. S., Winterwerp, J. C., Wang, Z.-Y., and Pu, Q. 2009a. Suspended sediment dynamics and morphodynamics in the Yellow River, China. Sedimentology, 56, 785–806.

Van Maren, D. S., Winterwerp, J. C., Wu, B. S., and Zhou, J. J. 2009b. Numerical modelling of hyperconcentrated flow in the Yellow River, China. Earth Surf. Processes Landforms, 34, 596–612.

Van Maren, D.S., Van Kessel, T., Cronin, K. and Sittoni, L., 2015a. The impact of channel deepening on estuarine sediment concentration. Continental Shelf Research, Vol. 95, 1-14

Van Maren, D.S., Winterwerp, J.C., and Vroom, J., 2015b. Fine sediment transport into the hyper-turbid lower Ems River: the role of channel deepening and sediment-induced drag reduction. Ocean Dynamics, DOI 10, 1007/s/10236-015-0821-2

Van Os, A.G., 1993. Density currents and salt intrusion. Lecture notes UNESCO-IHE Institue for Water Education, Delft, The Netherlands

Van Rijn, L.C., 1984a. Sediment Transport, Part I: Bed Load Transport. Journal of Hydraulic Engineering, ASCE, Vol. 110, No. 10.

Van Rijn, L.C., 1984b. Sediment Transport, Part II: Suspended Load Transport. Journal of Hydraulic Engineering, ASCE, Vol. 110, No. 11.

Van Rijn, L.C., 1993. Principles of sediment transport in rivers, estuaries and coastal seas. www.aquapublications.nl

Van Rijn, L.C., 2007. Unified view of sediment transport by currents and waves, I, II, III. ASCE, Journal of Hydraulic Engineering, Vol. 133, No. 6, 649-667, 668-689, No. 7, 761-775

Van Rijn, L.C., 2011. Principles of fluid flow and surface waves in rivers, estuaries and coastal seas. www.aquapublications.nl

Van Rijn 2015. Principles of sedimentation and erosion engineering in rivers, estuaries and coastal seas. www.aquapublications.nl

Van Straaten, L.M. and Kuenen, J.U., 1957. Accumulatioin of fine-grained sediments in the Dutch Wadden Sea. Geologie Mijnbouw, Vol. 19, 329-354

Vinzon, S.B. and Mehta, A.J., 2003. Lutoclines in high concentration estuaries: some observations at the Mouth of the Amazon. Journal of Coastal Research, Vol. 19, No. 2, 243-253

Walther, R., Schaguene, J., Hamm, L. and David, E., 2012. Coupled 3D modeling of turbidity maximum dynamics in the Loire estuary, France. Coastal Engineering Proc. 1 (33) (sediment-22).

Winterwerp, J.C., 2001. Stratification effects by cohesive and non cohesive sediment. Journal of Geophysical Research, Vol. 106, No C10, 22,559-22,574

Winterwerp, J.C. 2006. Stratification effects by fine suspended sediment at low, medium and very high concentrations.J. Geophys. Res. 111(C5, doi:10.1029/2005JC003019).

Winterwerp, J.C., 2011. Fine sediment transport by tidal asymmetry in the high- concentrated Ems River: indications for a regime shift in response to channel deepening. Ocean Dynamics, Vol. 61, 203–215.

Winterwerp, J.C. and Van Kessel, T., 2003. Siltation by sediment-induced density currents. Ocean Dynamics 53, 186-196.

Winterwerp, J.C. and Wang, Z.B., 2013. Man-induced regime shifts in small estuaries-I: theory. Ocean Dynamics, DOI10.1007/s10236-013-0662-9

Winterwerp, J.C., Wang, Z.B., Van Braeckel, A., Van Holland, G. and Kösters, F., 2013. Man-induced regime shifts in small estuaries-Part II: a comparison of rivers. Ocean Dynamics, Vol 63 (11–12), 1293–1306.

Xu, J., 1999a. Grain-size characteristics of suspended sediment in the Yellow River, China. Catena, Vol. 38, 243-263

Xu, J., 1999b. Erosion caused by hyperconcentrated flow on the Loess Plateau of China. Catena, Vol. 36, 1-19